Chapter IV

Results and Discussions

This chapter discusses the results obtained by damage and scale identification from both the vector sum algorithm and the ellipse fit algorithm. Since there are two kinds of casing shape, circular and ellipse, these casing shapes have an effect on damage and scale identification. We will show an advantage and disadvantage of both algorithms affected by the casing shape.

Since the data used to process are huge in volume, we cannot show them all in this paper. Table 4.1 depicts measurements of 72 casing radii measured at different depths for two measurement runs in the case of circular casing. The data shown in the table are used to demonstrate the casing wear when the vector sum and ellipse fit algorithms are used to process the data.

Table 4.2 shows measurements of 72 casing radii at different depths of two measurement runs in the case of oval casing. The data shown in the table are used to demonstrate the casing wear when the vector sum and ellipse fit algorithms are used to process the data.

Table 4.1: Radii measurements obtained in Run 1 and Run 2 in case of circular casing.

Position	Run 1				Run 2			
	Depth (ft)				Depth (ft)			
	2010.0	2009.5	2009.0	2008.5	2010.0	2009.5	2009.0	2008.5
1	4.4076	4.4069	4.4178	4.3977	4.4421	4.4341	4.4404	4.4357
2	4.4120	4.4201	4.4177	4.4230	4.4360	4.4367	4.4337	4.4530
3	4.4245	4.4310	4.4236	4.3992	4.4380	4.4333	4.4348	4.4473
4	4.4154	4.4155	4.4217	4.4162	4.4376	4.4430	4.4558	4.4529
5	4.4009	4.4100	4.4171	4.3961	4.4548	4.4415	4.4485	4.4405
6	4.4050	4.4136	4.4148	4.4286	4.4446	4.4537	4.4442	4.4589
7	4.4115	4.4270	4.4154	4.4062	4.4316	4.4360	4.4268	4.4396
8	4.4077	4.4110	4.4112	4.4124	4.4251	4.4271	4.4474	4.4414
9	4.4106	4.4193	4.4177	4.3894	4.4429	4.4232	4.4303	4.4254
10	4.4219	4.4251	4.4185	4.4302	4.4354	4.4415	4.4354	4.4344
11	4.4244	4.4358	4.4259	4.4204	4.4177	4.4258	4.4146	4.4215
12	4.4187	4.4174	4.4169	4.4259	4.4077	4.4135	4.4249	4.4267
13	4.4220	4.4306	4.4244	4.4017	4.4259	4.4037	4.4098	4.4085
14	4.4331	4.4294	4.4263	4.4482	4.4212	4.4239	4.4206	4.4137
15	4.4309	4.4355	4.4290	4.4282	4.4055	4.4143	4.4066	4.4013
16	4.4270	4.4164	4.4239	4.4288	4.4024	4.4097	4.4085	4.4205
17	4.4265	4.4318	4.4253	4.4137	4.4142	4.3992	4.3982	4.4059
18	4.4332	4.4190	4.4172	4.4506	4.4186	4.4184	4.4234	4.4026
19	4.4227	4.4323	4.4203	4.4210	4.4044	4.4163	4.4086	4.3967
20	4.4142	4.4097	4.4188	4.4231	4.4109	4.4236	4.4042	4.4186
21	4.4152	4.4184	4.4138	4.4119	4.4222	4.4118	4.4113	4.4149
22	4.4247	4.4110	4.4018	4.4349	4.4184	4.4138	4.4285	4.4064
23	4.4099	4.4168	4.4040	4.4088	4.3984	4.4129	4.4134	4.4014
24	4.4053	4.4034	4.4137	4.4135	4.4111	4.4206	4.4008	4.4156
25	4.4081	4.4109	4.4062	4.4076	4.4164	4.4155	4.4132	4.4143
26	4.4184	4.4092	4.3915	4.4199	4.4070	4.4066	4.4217	4.4100
27	4.4092	4.4191	4.4048	4.4020	4.4015	4.4140	4.4132	4.4054
28	4.4075	4.4055	4.4188	4.4149	4.4112	4.4218	4.4035	4.4114
29	4.4098	4.4115	4.4079	4.4104	4.4120	4.4197	4.4134	4.4167
30	4.4278	4.4220	4.4028	4.4159	4.3964	4.4018	4.4175	4.4164
31	4.4180	4.4281	4.4238	4.4097	4.4040	4.4074	4.4061	4.4117
32	4.4227	4.4176	4.4341	4.4197	4.4093	4.4091	4.4030	4.4876
33	4.4226	4.4209	4.4224	4.4200	4.4122	4.4254	4.5025	4.5037
34	4.4287	4.4305	4.4078	4.4165	4.4118	4.4935	4.5061	4.4291
35	4.4135	4.4270	4.4296	4.4210	4.5095	4.4985	4.4187	4.4356
36	4.4135	4.4113	4.4288	4.4191	4.5043	4.4151	4.4217	4.4260

Table 4.1: Radii measurements obtained in Run 1 and Run 2 in case of circular casing (continued).

Position	Run 1				Run 2			
	Depth (ft)				Depth (ft)			
	2010.0	2009.5	2009.0	2008.5	2010.0	2009.5	2009.0	2008.5
37	4.4102	4.4100	4.4101	4.4189	4.4246	4.4374	4.4379	4.4406
38	4.4191	4.4169	4.4021	4.4032	4.4278	4.4365	4.4412	4.4425
39	4.4062	4.4134	4.4219	4.4211	4.4467	4.4335	4.4314	4.4229
40	4.4132	4.4117	4.4210	4.4129	4.4350	4.4184	4.4481	4.4341
41	4.4096	4.4110	4.4152	4.4203	4.4330	4.4356	4.4377	4.4474
42	4.4101	4.4110	4.4003	4.3973	4.4312	4.4339	4.4380	4.4408
43	4.4012	4.3998	4.4163	4.4211	4.4459	4.4378	4.4269	4.4169
44	4.4092	4.4142	4.4147	4.4093	4.4246	4.4136	4.4356	4.4303
45	4.4107	4.4086	4.4161	4.4188	4.4164	4.4173	4.4194	4.4386
46	4.4195	4.4206	4.4152	4.3942	4.4209	4.4201	4.4163	4.4222
47	4.4204	4.4109	4.4205	4.4293	4.4326	4.4298	4.4171	4.4030
48	4.4287	4.4345	4.4346	4.4240	4.4128	4.4025	4.4175	4.4129
49	4.4315	4.4317	4.4314	4.4422	4.4045	4.4098	4.4090	4.4234
50	4.4343	4.4394	4.4322	4.4130	4.4100	4.4100	4.4012	4.4116
51	4.4344	4.4210	4.4299	4.4424	4.4260	4.4288	4.4105	4.4023
52	4.4362	4.4440	4.4384	4.4396	4.4131	4.4033	4.4171	4.4103
53	4.4380	4.4373	4.4344	4.4523	4.4038	4.4095	4.4080	4.4173
54	4.4284	4.4408	4.4360	4.4163	4.4096	4.4095	4.3993	4.4137
55	4.4288	4.4129	4.4173	4.4483	4.4259	4.4339	4.4185	4.4150
56	4.4279	4.4358	4.4269	4.4305	4.4198	4.4168	4.4276	4.4158
57	4.4271	4.4219	4.4154	4.4397	4.4187	4.4281	4.4290	4.4258
58	4.4181	4.4268	4.4277	4.4126	4.4173	4.4177	4.4063	4.4279
59	4.4155	4.4094	4.4135	4.4334	4.4198	4.4247	4.4221	4.4194
60	4.4162	4.4218	4.4071	4.4250	4.4099	4.4123	4.4175	4.4108
61	4.4202	4.4137	4.4085	4.4163	4.4082	4.4186	4.4190	4.4115
62	4.4048	4.4140	4.4191	4.4082	4.4011	4.4085	4.3991	4.4224
63	4.4113	4.4051	4.4104	4.4211	4.4086	4.4133	4.4163	4.4206
64	4.4122	4.4154	4.3973	4.4164	4.3971	4.3985	4.4062	4.4112
65	4.4200	4.4096	4.4039	4.4064	4.4125	4.4171	4.4161	4.4076
66	4.4067	4.4082	4.4151	4.4036	4.4015	4.4079	4.4033	4.4177
67	4.4170	4.4149	4.4183	4.4131	4.4008	4.4072	4.4122	4.4163
68	4.4167	4.4228	4.3955	4.4185	4.3936	4.3945	4.4008	4.4132
69	4.4288	4.4220	4.4168	4.3989	4.4196	4.4135	4.4120	4.4055
70	4.4113	4.4160	4.4211	4.4153	4.4125	4.4196	4.4175	4.4167
71	4.4209	4.4208	4.4237	4.4151	4.4190	4.4213	4.4305	4.4336
72	4.4168	4.4209	4.3934	4.4235	4.4198	4.4168	4.4212	4.4384

Table 4.2: Radii measurements obtained in Run 1 and Run 2 in case of oval casing.

Position	Run 1				Run 2			
	Depth (ft)				Depth (ft)			
	3010.0	3009.5	3009.0	3008.5	3010.0	3009.5	3009.0	3008.5
1	4.3154	4.3055	4.2982	4.3023	4.3560	4.3169	4.3249	4.3639
2	4.3478	4.3696	4.3499	4.3325	4.3394	4.3320	4.3195	4.3104
3	4.3142	4.3090	4.3015	4.3117	4.3777	4.3196	4.3048	4.3132
4	4.3018	4.3873	4.3410	4.3594	4.3808	4.3443	4.3697	4.3691
5	4.3605	4.3470	4.3732	4.3075	4.3464	4.3596	4.3406	4.3883
6	4.3592	4.3960	4.3771	4.3357	4.3817	4.3642	4.4038	4.3690
7	4.3808	4.3644	4.3427	4.3450	4.3511	4.3747	4.3447	4.3984
8	4.3770	4.3620	4.3669	4.3991	4.3561	4.4038	4.3975	4.3583
9	4.3618	4.3632	4.4184	4.3591	4.4125	4.3519	4.4178	4.4080
10	4.3811	4.4133	4.4083	4.4050	4.3670	4.4374	4.3836	4.3921
11	4.4314	4.3749	4.3948	4.4361	4.4315	4.4282	4.4012	4.3590
12	4.4592	4.3744	4.4526	4.3978	4.3924	4.3842	4.4288	4.4086
13	4.4131	4.4083	4.4341	4.3813	4.4282	4.4356	4.4018	4.4536
14	4.4308	4.4520	4.4535	4.4450	4.4077	4.4665	4.4620	4.3891
15	4.4339	4.4018	4.4386	4.4645	4.3931	4.4638	4.4463	4.4251
16	4.4089	4.4100	4.4135	4.4711	4.4276	4.4110	4.4472	4.4501
17	4.4835	4.4358	4.4075	4.4201	4.4782	4.4032	4.4069	4.4362
18	4.4627	4.4188	4.4443	4.4003	4.4202	4.4753	4.4162	4.4651
19	4.4826	4.4480	4.4636	4.4242	4.4834	4.4775	4.4577	4.4328
20	4.4024	4.3994	4.4389	4.4262	4.5401	4.4147	4.4015	4.4196
21	4.4081	4.3980	4.4198	4.3821	4.5207	4.5481	4.4537	4.3769
22	4.3945	4.4430	4.4410	4.3817	4.4372	4.5540	4.5513	4.3969
23	4.3779	4.4560	4.4397	4.3623	4.3849	4.4150	4.5028	4.5112
24	4.3888	4.4120	4.3763	4.3973	4.3889	4.3858	4.4258	4.5122
25	4.3695	4.3830	4.4322	4.3834	4.4238	4.3650	4.3782	4.3957
26	4.3503	4.4011	4.4190	4.3611	4.4217	4.3895	4.3614	4.4238
27	4.3883	4.3905	4.3743	4.3575	4.3976	4.3681	4.4012	4.3426
28	4.3840	4.3809	4.3861	4.3780	4.3754	4.3470	4.3664	4.4003
29	4.3746	4.3721	4.3709	4.3950	4.3851	4.3557	4.3937	4.3605
30	4.3936	4.3142	4.3549	4.3641	4.3147	4.3939	4.3753	4.3308
31	4.3699	4.3457	4.3663	4.3854	4.3318	4.3548	4.3793	4.3290
32	4.3799	4.3030	4.3787	4.3285	4.3242	4.3200	4.3089	4.3129
33	4.3017	4.3727	4.3104	4.3604	4.3335	4.3622	4.3713	4.3047
34	4.2985	4.3738	4.2911	4.3537	4.3338	4.2960	4.2950	4.3494
35	4.3290	4.3599	4.2976	4.3323	4.3126	4.3285	4.3466	4.3331
36	4.3425	4.3103	4.3683	4.3372	4.3643	4.3669	4.3035	4.3547

Table 4.2: Radii measurements obtained in Run 1 and Run 2 in case of oval casing (continued).

Position	Run 1				Run 2			
	Depth (ft)				Depth (ft)			
	3010.0	3009.5	3009.0	3008.5	3010.0	3009.5	3009.0	3008.5
37	4.3283	4.3668	4.3597	4.3177	4.3584	4.3672	4.3398	4.3344
38	4.3225	4.3008	4.3289	4.3480	4.3132	4.3198	4.2993	4.3139
39	4.3784	4.3796	4.3018	4.3024	4.3087	4.3382	4.3482	4.3476
40	4.3058	4.3159	4.3201	4.3786	4.3638	4.3145	4.3861	4.3446
41	4.3358	4.3591	4.3452	4.3223	4.3190	4.3785	4.3776	4.3379
42	4.3870	4.3951	4.3497	4.3255	4.3250	4.3743	4.3286	4.3739
43	4.3284	4.3587	4.3408	4.3873	4.3267	4.3477	4.3370	4.3373
44	4.3782	4.3360	4.3901	4.3553	4.4008	4.3880	4.3548	4.3454
45	4.4047	4.3668	4.3949	4.3854	4.4023	4.3494	4.3526	4.3639
46	4.4306	4.3626	4.3762	4.3848	4.3693	4.4403	4.3633	4.4282
47	4.3762	4.4069	4.4296	4.4283	4.3701	4.4119	4.4131	4.4334
48	4.4299	4.3752	4.4530	4.4477	4.3761	4.4215	4.4281	4.4381
49	4.3804	4.4553	4.4241	4.4280	4.4569	4.4297	4.4494	4.4548
50	4.4395	4.4400	4.4625	4.3814	4.3927	4.4076	4.4372	4.4567
51	4.4301	4.4287	4.4459	4.4211	4.4051	4.3994	4.4760	4.3805
52	4.4466	4.4737	4.4382	4.4187	4.4201	4.4231	4.4450	4.4245
53	4.4081	4.4183	4.4817	4.3923	4.4206	4.4842	4.4591	4.4369
54	4.4830	4.4210	4.4556	4.4336	4.4524	4.4656	4.4581	4.4270
55	4.4610	4.4011	4.4499	4.3997	4.4786	4.4724	4.4235	4.4120
56	4.4602	4.3966	4.3968	4.4062	4.4412	4.4378	4.4631	4.4584
57	4.4707	4.4574	4.4667	4.4237	4.4230	4.4280	4.4348	4.4504
58	4.4257	4.3822	4.4393	4.4214	4.4376	4.3872	4.4200	4.3982
59	4.4527	4.3859	4.4150	4.4154	4.4568	4.4591	4.4117	4.3750
60	4.3941	4.4242	4.3692	4.3633	4.3674	4.4410	4.4423	4.3823
61	4.4065	4.4039	4.3750	4.4050	4.4092	4.4210	4.4022	4.3567
62	4.4046	4.3695	4.3992	4.4230	4.3927	4.3595	4.3683	4.4086
63	4.3616	4.3427	4.3772	4.4171	4.4054	4.3709	4.4009	4.4174
64	4.4070	4.3623	4.3312	4.4036	4.3781	4.3351	4.3400	4.3750
65	4.3905	4.3687	4.3736	4.3786	4.4064	4.3897	4.3818	4.3672
66	4.3231	4.3586	4.3555	4.3617	4.3721	4.3872	4.3358	4.3741
67	4.3275	4.3479	4.3451	4.3748	4.3645	4.3435	4.3165	4.3274
68	4.3144	4.3080	4.3439	4.3717	4.3593	4.3331	4.3549	4.3350
69	4.3504	4.3566	4.3494	4.3257	4.3447	4.3688	4.3169	4.3526
70	4.3198	4.2953	4.3354	4.3000	4.3415	4.3186	4.3136	4.3184
71	4.3004	4.3698	4.3693	4.3630	4.3112	4.3357	4.3335	4.2953
72	4.2954	4.3677	4.3575	4.3058	4.3006	4.2950	4.3662	4.3351

4.1 The Vector Sum

Since the tool is not at the center of the casing, this offset causes an eccentricity. Thus, the vector sum plays a role to eliminate this eccentricity. The vector sum algorithm processes the data to calculate the corrected radii. Then, the casing damage or scale precipitation is located by subtracting the corrected radii from the average radius.

4.1.1 The corrected radii

The first step of the vector sum algorithm is to calculate the center of the casing. Sample calculations are performed using the measurements at depth 2010.0 ft from Table 4.1. The value of R_{CXi}, R_{CYi}, and R_{Ci} (the corrected radii) can be calculated using Eq. 2.18, Eq. 2.19 and Eq. 2.20, respectively as shown in Table 4.3. Also shown in the table is the difference between the corrected radii and the average radius.

The summation of the radius shown in column 3 of Table 4.2 over 72 positions is 318.1061. The average radius is then

$$R_{avg} = 318.1061 / 72 = 4.418 \tag{4.1}$$

The summation of the $R\cos\theta$ in column 4 of Table 4.2 over 72 positions is

$$\sum_{i=1}^{72} R_i \cos\theta_i = -0.00602 \tag{4.2}$$

And the summation of the $R\sin\theta$ in column 5 of Table 4.2 over 72 positions is

$$\sum_{i=1}^{72} R_i \sin\theta_i = -0.06502 \tag{4.3}$$

Substituting Eq. 4.2 into Eq. 2.13, we get

$$V_{CX} = \frac{-0.00602}{72} = -8.36\text{E}-05 \tag{4.4}$$

Table 4.3: Finding the corrected radii and the damage.

Position	Angle(θ)	R	$R\cos\theta$	$R\sin\theta$	R_{CX}	R_{CY}	R_C	R_{avg}-R_C
1	5	4.408	4.391	0.384	4.391	0.384	4.408	0.0107
2	10	4.412	4.345	0.766	4.345	0.766	4.412	0.0064
3	15	4.425	4.274	1.145	4.274	1.145	4.425	-0.0060
4	20	4.415	4.149	1.510	4.149	1.510	4.415	0.0031
5	25	4.401	3.989	1.860	3.989	1.860	4.401	0.0176
6	30	4.405	3.815	2.203	3.815	2.203	4.405	0.0137
7	35	4.412	3.614	2.530	3.614	2.530	4.412	0.0072
8	40	4.408	3.376	2.833	3.376	2.833	4.408	0.0110
9	45	4.411	3.119	3.119	3.119	3.119	4.411	0.0083
10	50	4.422	2.842	3.387	2.842	3.387	4.422	-0.0030
11	55	4.424	2.538	3.624	2.538	3.624	4.424	-0.0055
12	60	4.419	2.209	3.827	2.209	3.827	4.419	0.0003
13	65	4.422	1.869	4.008	1.869	4.008	4.422	-0.0030
14	70	4.433	1.516	4.166	1.516	4.166	4.433	-0.0141
15	75	4.431	1.147	4.280	1.147	4.280	4.431	-0.0119
16	80	4.427	0.769	4.360	0.769	4.360	4.427	-0.0080
17	85	4.427	0.386	4.410	0.386	4.410	4.427	-0.0075
18	90	4.433	0.000	4.433	0.000	4.433	4.433	-0.0141
19	95	4.423	-0.385	4.406	-0.385	4.406	4.423	-0.0037
20	100	4.414	-0.767	4.347	-0.767	4.347	4.414	0.0049
21	105	4.415	-1.143	4.265	-1.143	4.265	4.415	0.0038
22	110	4.425	-1.513	4.158	-1.513	4.158	4.425	-0.0057
23	115	4.410	-1.864	3.997	-1.864	3.997	4.410	0.0090
24	120	4.405	-2.203	3.815	-2.203	3.815	4.405	0.0136
25	125	4.408	-2.528	3.611	-2.528	3.611	4.408	0.0107
26	130	4.418	-2.840	3.385	-2.840	3.385	4.418	0.0004
27	135	4.409	-3.118	3.118	-3.118	3.118	4.409	0.0095
28	140	4.408	-3.376	2.833	-3.376	2.833	4.408	0.0111
29	145	4.410	-3.612	2.529	-3.612	2.529	4.410	0.0088
30	150	4.428	-3.835	2.214	-3.835	2.214	4.428	-0.0093
31	155	4.418	-4.004	1.867	-4.004	1.867	4.418	0.0004
32	160	4.423	-4.156	1.513	-4.156	1.513	4.423	-0.0044
33	165	4.423	-4.272	1.145	-4.272	1.145	4.423	-0.0043
34	170	4.429	-4.361	0.769	-4.361	0.769	4.429	-0.0104
35	175	4.414	-4.397	0.385	-4.397	0.385	4.414	0.0047
36	180	4.414	-4.414	0.000	-4.414	0.000	4.414	0.0046

Table 4.3: Finding the corrected radii and the damage (continued).

Position	Angle(θ)	R	$R\cos\theta$	$R\sin\theta$	R_{CX}	R_{CY}	R_C	R_{avg}-R_C
37	185	4.410	-4.393	-0.384	-4.393	-0.384	4.410	0.0078
38	190	4.419	-4.352	-0.767	-4.352	-0.767	4.419	-0.0011
39	195	4.406	-4.256	-1.140	-4.256	-1.140	4.406	0.0116
40	200	4.413	-4.147	-1.509	-4.147	-1.509	4.413	0.0045
41	205	4.410	-3.996	-1.864	-3.996	-1.864	4.410	0.0081
42	210	4.410	-3.819	-2.205	-3.819	-2.205	4.410	0.0075
43	215	4.401	-3.605	-2.524	-3.605	-2.524	4.401	0.0164
44	220	4.409	-3.378	-2.834	-3.378	-2.834	4.409	0.0083
45	225	4.411	-3.119	-3.119	-3.119	-3.119	4.411	0.0068
46	230	4.420	-2.841	-3.386	-2.841	-3.386	4.420	-0.0021
47	235	4.420	-2.535	-3.621	-2.535	-3.621	4.420	-0.0030
48	240	4.429	-2.214	-3.835	-2.214	-3.835	4.429	-0.0114
49	245	4.432	-1.873	-4.016	-1.873	-4.016	4.432	-0.0142
50	250	4.434	-1.517	-4.167	-1.517	-4.167	4.434	-0.0170
51	255	4.434	-1.148	-4.283	-1.148	-4.283	4.434	-0.0171
52	260	4.436	-0.770	-4.369	-0.770	-4.369	4.436	-0.0190
53	265	4.438	-0.387	-4.421	-0.387	-4.421	4.438	-0.0208
54	270	4.428	0.000	-4.428	0.000	-4.428	4.428	-0.0112
55	275	4.429	0.386	-4.412	0.386	-4.412	4.429	-0.0116
56	280	4.428	0.769	-4.361	0.769	-4.361	4.428	-0.0106
57	285	4.427	1.146	-4.276	1.146	-4.276	4.427	-0.0098
58	290	4.418	1.511	-4.152	1.511	-4.152	4.418	-0.0008
59	295	4.416	1.866	-4.002	1.866	-4.002	4.416	0.0019
60	300	4.416	2.208	-3.825	2.208	-3.825	4.416	0.0012
61	305	4.420	2.535	-3.621	2.535	-3.621	4.420	-0.0028
62	310	4.405	2.831	-3.374	2.831	-3.374	4.405	0.0127
63	315	4.411	3.119	-3.119	3.119	-3.119	4.411	0.0063
64	320	4.412	3.380	-2.836	3.380	-2.836	4.412	0.0054
65	325	4.420	3.621	-2.535	3.621	-2.535	4.420	-0.0024
66	330	4.407	3.816	-2.203	3.816	-2.203	4.407	0.0111
67	335	4.417	4.003	-1.867	4.003	-1.867	4.417	0.0009
68	340	4.417	4.150	-1.511	4.150	-1.511	4.417	0.0012
69	345	4.429	4.278	-1.146	4.278	-1.146	4.429	-0.0108
70	350	4.411	4.344	-0.766	4.344	-0.766	4.411	0.0067
71	355	4.421	4.404	-0.385	4.404	-0.385	4.421	-0.0028
72	360	4.417	4.417	0.000	4.417	0.000	4.417	0.0014

Substituting Eq. 4.3 into Eq. 2.14

$$V_{CY} = \frac{-0.06502}{72} = -9.03\,\mathrm{E}-04 \tag{4.5}$$

Then, the angle of the correcting vector can be computed as

$$\tan\beta = \frac{\sum_{i=1}^{72} V_{BY\,i}}{\sum_{i=1}^{72} V_{BX\,i}} = \frac{-0.06502}{-0.00602} \tag{4.6}$$

$$\beta = 264.7 \tag{4.7}$$

The center of the tool can be corrected by the vector $-8.36\text{x}10^{-05}$i $-9.03\text{x}10^{-04}$j. In another word, the center of the circle is at ($-8.36\text{x}10^{-05}$, $-9.03\text{x}10^{-04}$) as shown in Fig. 4.1.

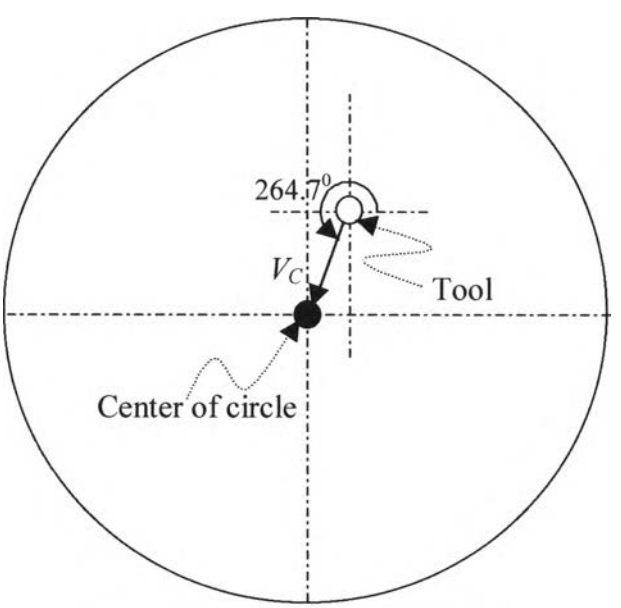

Figure 4.1: The center of the circle.

From Eq. 2.18 and Eq. 2.19, we can calculate the corrected radii in x and y component respectively as shown in column 6 and 7 of Table 4.2. Then, we can calculate the corrected radii from Eq. 2.20 as shown in column 8 in Table 4.2.

4.1.2 Damage and scale identification

We can determine the location of damage and scale precipitation by subtracting the corrected radii (column 8 of Table 4.2) at each depth from the average radius (from Eq. 4.1) as shown in column 9 of Table 4.2. Then, the differences between the corrected radii and the average radius are plotted up using the function "imagesc" in MATLAB.

As mentioned before, the casing shape is classified to circular and oval casing. We divide the damage and scale identification into 2 cases as follows:

(a) Circular casing

Case 1a: No casing damage and scale precipitation

The vector sum algorithm was used to process the measurements in Run 1 shown in Table 4.1 when the casing shape is circular. The differences between the corrected radii and the average radius are shown in Fig. 4.2. As seen in the figures, there is no casing damage and scale precipitation during Run 1.

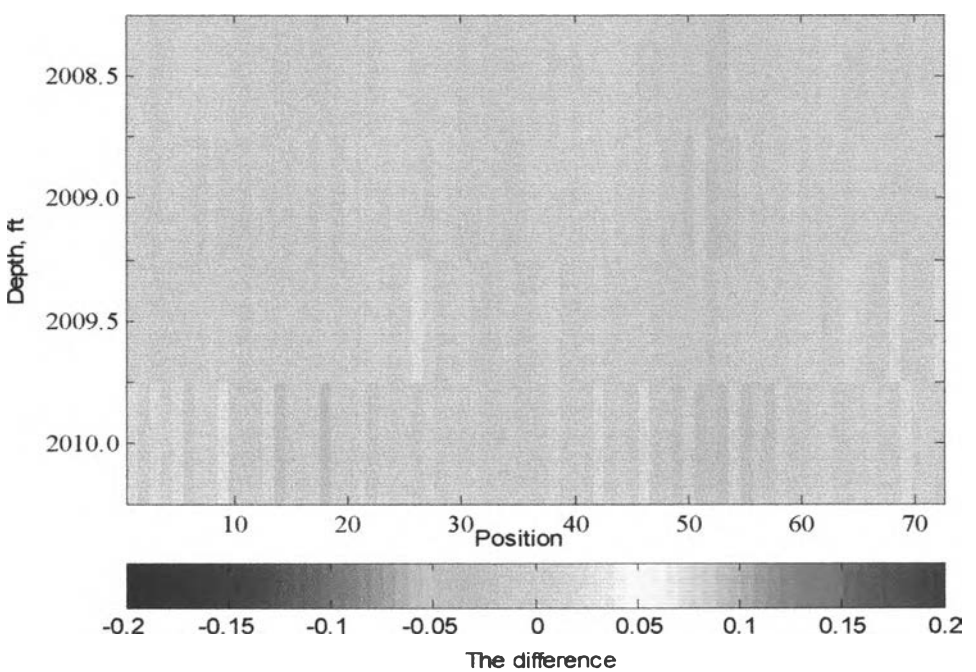

Figure 4.2: Damage and scale identification of Run 1 processed by the vector sum algorithm (circular casing).

Case 2a: Casing is damaged

The vector sum algorithm was used to process the measurements in Run 2 shown in Table 4.1 when the casing shape is circular. The differences between the corrected radii and the average radius are shown in Fig. 4.3. As seen in the figures, there is a damage in the second run.

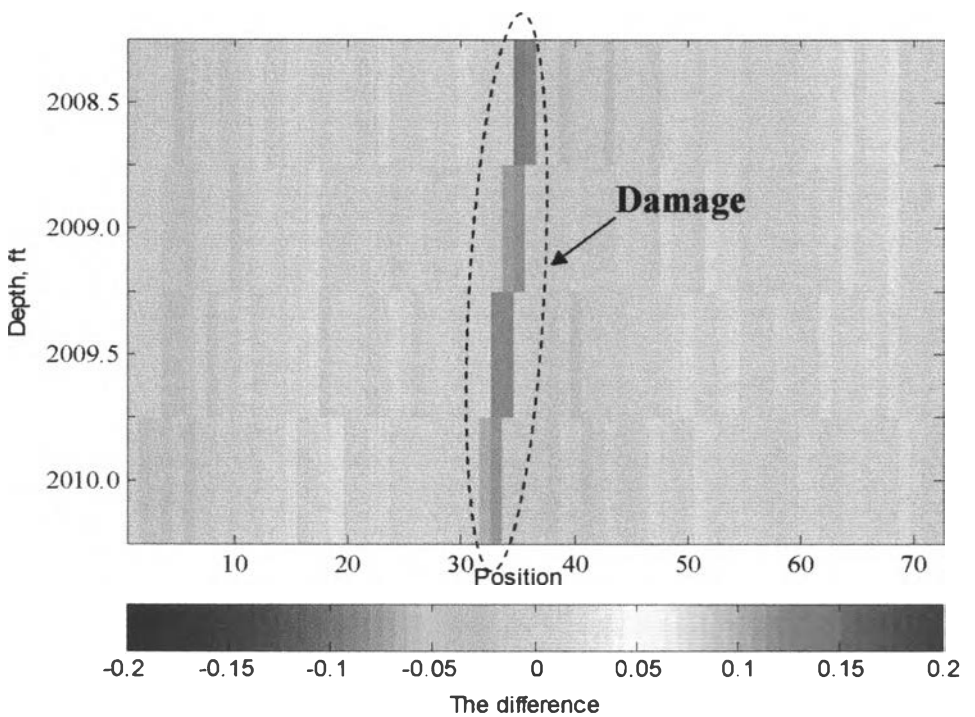

Figure 4.3: Damage and scale identification of Run 2 processed by the vector sum algorithm (circular casing).

(b) Oval casing

Case 1b: No casing damage and scale precipitation

The vector sum algorithm was used to process the measurements in Run 1 shown in Table 4.2 when the casing shape is oval. The differences between the corrected radii and the average radius are shown in Fig. 4.4.

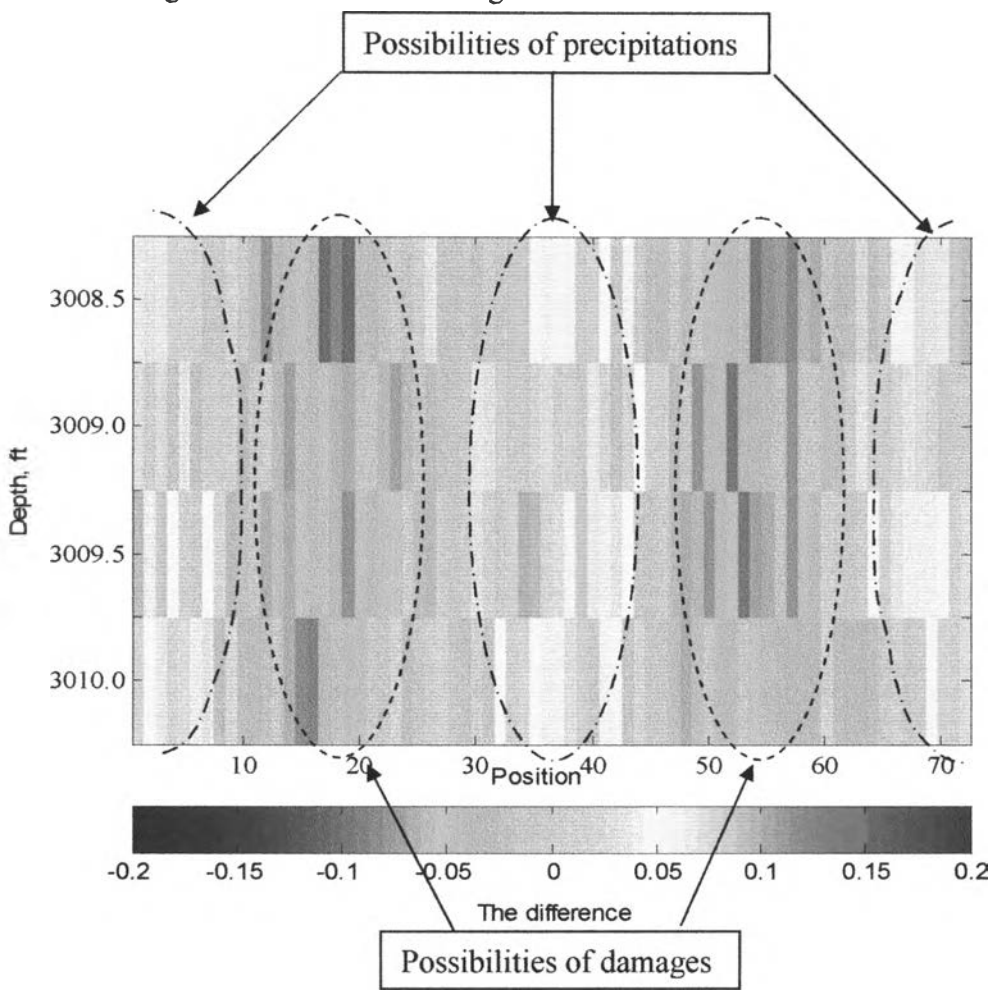

Figure 4.4: Damage and scale identification of Run 1 processed by the vector sum algorithm (oval casing).

As shown in Fig. 4.4, the vector sum algorithm identifies two striped damages (blue color zone) and two precipitations (yellow color zone). Actually, there are no damages and precipitations on the casing. The erroneous differences between the raw radii and the average radius simply result from the differences between the actual shape of the casing and the circular shape assumed in the vector sum algorithm. Since it incorrectly identifies casing damages and precipitations, the vector sum algorithm is not suitable for an oval casing.

Case 2b: Casing is damaged

The vector sum algorithm was used to process the measurements in Run 2 shown in Table 4.2 when the casing shape is oval. The differences between the corrected radii and the average radius are shown in Fig, 4.5.

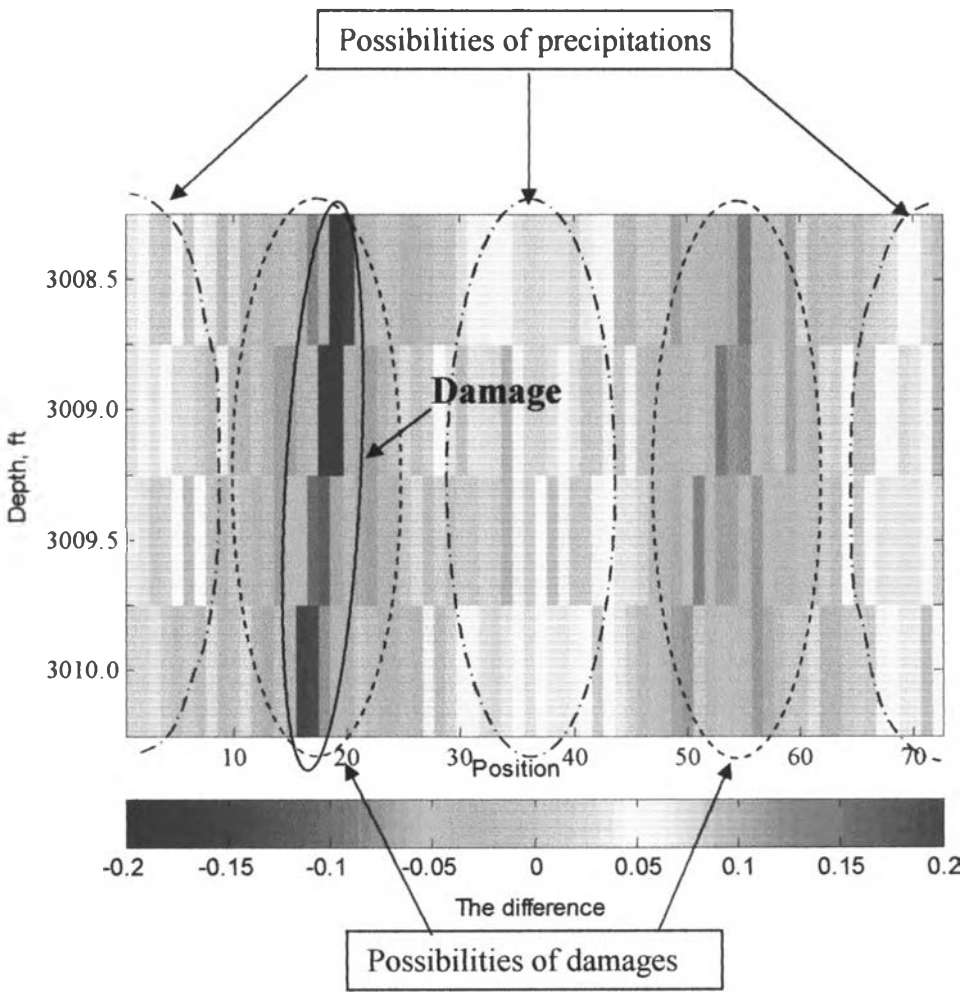

Figure 4.5: Damage and scale identification of Run 2 processed by the vector sum algorithm (oval casing).

Fig. 4.5 shows one obvious damage, two possibilities of damages and two possibilities of precipitations. Since the vector sum algorithm assumes that the casing is round and that the measured radii lie on a circle, the two striped damages and precipitations are just artifacts from the assumption.

When casing is under stress and strain of different magnitudes, the actual shape of a casing looks like an ellipse rather than a circle. In this case, the vector sum may incorrectly identify damage and precipitation. The reason for such false identification can be explained using Fig. 4.6.

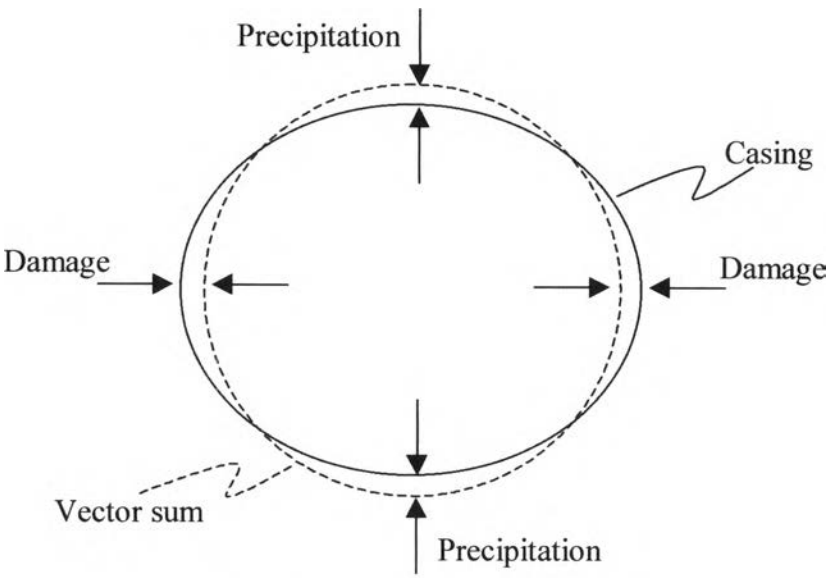

Figure 4.6: The vector sum shows the error.

In this case, the casing shape is actually elliptic but the vector sum assumes it to be a circle. When the differences between the data (ellipse) and the vector sum (circle) are identified, it seems like there are casing damages and precipitations. These errors result from the assumption that the casing has a circular shape. This problem can be solved when using the ellipse fit algorithm.

4.2 The Ellipse Fit

When the ellipse fit algorithm is used to process the data, the coefficients of the fitted ellipse are calculated. The ellipticity can then be calculated from these coefficients. Then, the casing damage and scale precipitation can be identified. When two runs are taken, the measurements in these runs must be synchronized before the change in casing conditions can be determined.

4.2.1 The coefficients of ellipse

The coefficients *a, b, c, d, e* and *f* of ellipse are obtained from Eq. 2.43 as shown in Section 2.2.1. Eq. 2.43 is presented in term of rectangular coordinate but the data are shown in term of polar coordinate. Thus, the data are changed to the (x, y) coordinate system by

$$x = R\cos\theta \tag{4.8}$$

$$y = R\sin\theta \tag{4.9}$$

where

x is the data value in x-axis in rectangular coordinate.

y is the data value in y-axis in rectangular coordinate.

R is the radii in polar coordinate.

θ is the angle of data in polar coordinate.

The data at depth 2010.0 ft obtained in Run 1 and shown in Table 4.1 are used as an example to evaluate the coefficients *a, b, c, d, e* and *f* of ellipse step by step as follows:

1. Calculate the Design Matrix, ***D***.

$$\boldsymbol{D} = \begin{bmatrix} 19.279 & 1.687 & 0.148 & 4.391 & 0.384 & 1 \\ 18.878 & 3.329 & 0.587 & 4.345 & 0.766 & 1 \\ 18.265 & 4.894 & 1.311 & 4.274 & 1.145 & 1 \\ \bullet & \bullet & \bullet & \bullet & \bullet & \bullet \\ \bullet & \bullet & \bullet & \bullet & \bullet & \bullet \\ \bullet & \bullet & \bullet & \bullet & \bullet & \bullet \\ 18.873 & -3.328 & 0.587 & 4.344 & -0.766 & 1 \\ 19.396 & -1.697 & 0.148 & 4.404 & -0.385 & 1 \\ 19.508 & 0.000 & 0.000 & 4.417 & 0.000 & 1 \end{bmatrix}$$

2. Calculate the scatter matrix, S, by $S = D^T D$

$$S = \begin{bmatrix} 10{,}257.630 & -6.351 & 3420.520 & -0.436 & 0.074 & 701.718 \\ -6.351 & 3420.520 & 12.807 & 0.074 & 0.080 & 0.164 \\ 3420.520 & 12.807 & 10{,}336.110 & 0.080 & -3.891 & 0703.725 \\ -0.436 & 0.074 & 0.080 & 701.718 & 0.164 & -0.006 \\ 0.074 & 0.080 & -3.891 & 0.164 & 703.725 & -0.065 \\ 701.718 & 0.164 & 703.725 & -0.006 & -0.065 & 72.000 \end{bmatrix}$$

3. Calculate the lower triangular matrix, L.

$$L = \begin{bmatrix} 101.2800 & 0 & 0 & 0 & 0 & 0 \\ -0.0627 & 58.4852 & 0 & 0 & 0 & 0 \\ 33.7730 & 0.2552 & 95.8928 & 0 & 0 & 0 \\ -0.0043 & 0.0013 & 0.0023 & 26.4900 & 0 & 0 \\ 0.0007 & 0.0014 & -0.0408 & 0.0062 & 26.5278 & 0 \\ 6.9285 & 0.0102 & 4.8985 & 0.0005 & 0.0049 & 0.0300 \end{bmatrix}$$

4. Calculate the inverse matrix, L^{-1}.

$$L^{-1} = \begin{bmatrix} 0.0099 & 0 & 0 & 0 & 0 & 0 \\ 0.0000 & 0.0171 & 0 & 0 & 0 & 0 \\ -0.0035 & -0.0001 & 0.0104 & 0 & 0 & 0 \\ 0.0000 & 0.0000 & 0.0000 & 0.0378 & 0 & 0 \\ 0.0000 & 0.0000 & 0.0000 & 0.0000 & 0.0377 & 0 \\ -1.7121 & 0.0016 & -1.7024 & -0.0006 & -0.0062 & 33.3259 \end{bmatrix}$$

5. Calculate the matrix E where $E = (L^{-1} C (L^{-1})^T)$

$$E = \begin{bmatrix} 0.0000 & 0.0000 & -0.0002 & 0.0000 & 0.0000 & 0.0336 \\ 0.0000 & 0.0003 & 0.0000 & 0.0000 & 0.0000 & 0.0001 \\ -0.0002 & 0.0000 & 0.0002 & 0.0000 & 0.0000 & 0.0239 \\ 0.0000 & 0.0000 & 0.0000 & 0.0000 & 0.0000 & 0.0000 \\ 0.0000 & 0.0000 & 0.0000 & 0.0000 & 0.0000 & 0.0000 \\ 0.0336 & 0.0001 & 0.0239 & 0.0000 & 0.0000 & -11.6587 \end{bmatrix}$$

6. Calculate the eigenvalues (λ) and eigenvectors (V).

$\lambda_1 = 0.000066$; $V_1 = [0.7840 \quad 0.0000 \quad 0.6208 \quad 0.0002 \quad 0.0016 \quad 0.0035]$

$\lambda_2 = -0.00029$; $V_2 = [-0.0084 \quad 0.9999 \quad 0.0105 \quad -0.0001 \quad 0.0000 \quad 0.0000]$

$\lambda_3 = -0.00036$; $V_3 = [-0.6207 \quad -0.0134 \quad 0.7839 \quad -0.0001 \quad 0.0011 \quad -0.0002]$

$\lambda_4 = -0.00000$; $V_4 = [-0.0003 \quad 0.0001 \quad 0.0000 \quad 1.0000 \quad -0.0067 \quad 0.0000]$

$\lambda_5 = -0.00000$; $V_5 = [-0.0006 \quad 0.0001 \quad -0.00018 \quad 0.0067 \quad 1.0000 \quad 0.0000]$

$\lambda_6 = 116588$; $V_6 = [-0.0029 \quad 0.0000 \quad -0.0021 \quad 0.0000 \quad 0.0000 \quad 1.0000]$

7. Calculate the unnormalized eigenvectors, a.

$\lambda_1 = 0.000066$; $a_1 = [-0.0005 \quad 0.0000 \quad 0.0005 \quad 0.0000 \quad 0.0000 \quad 0.1177]$

$\lambda_2 = -0.00029$; $a_2 = [-0.0001 \quad 0.0171 \quad 0.0001 \quad 0.0000 \quad 0.0000 \quad 0.0001]$

$\lambda_3 = -0.00036$; $a_3 = [-0.0085 \quad -0.0003 \quad 0.0085 \quad 0.0000 \quad 0.0000 \quad -0.0062]$

$\lambda_4 = -0.00000$; $a_4 = [0.0000 \quad 0.0000 \quad 0.0000 \quad 0.0378 \quad -0.0003 \quad 0.0000]$

$\lambda_5 = -0.00000$; $a_5 = [0.0000 \quad 0.0000 \quad 0.0000 \quad 0.0002 \quad 0.0377 \quad -0.0001]$

$\lambda_6 = 116588$; $a_6 = [-1.7121 \quad 0.0016 \quad -1.7024 \quad -0.0006 \quad -0.0062 \quad 33.3256]$

8. Calculate the unit eigenvectors.

$\lambda_1 = 0.000066$; $a_1 = [-0.00395 \quad -0.00019 \quad 0.00393 \quad 0.00005 \quad 0.00033 \quad 0.99998]$

$\lambda_2 = -0.00029$; $a_2 = [-0.00664 \quad 0.99994 \quad 0.00614 \quad -0.00011 \quad -0.00009 \quad 0.00573]$

$\lambda_3 = -0.00036$; $a_3 = [-0.63099 \quad -0.01965 \quad 0.62742 \quad -0.00036 \quad 0.00302 \quad -0.45585]$

$\lambda_4 = -0.00000$; $a_4 = [0.00001 \quad 0.00000 \quad -0.00001 \quad 0.99998 \quad -0.00668 \quad -0.00043]$

$\lambda_5 = -0.00000$; $a_5 = [-0.00003 \quad 0.00000 \quad 0.00003 \quad 0.00646 \quad 0.99998 \quad -0.00214]$

$\lambda_6 = 116588$; $a_6 = [-0.05124 \quad 0.00005 \quad -0.05095 \quad -0.00002 \quad -0.00018 \quad 0.99739]$

9. Select the positive eigenvalue which is $\lambda_6 = 11.6588$. Then, the eigenvector corresponding to the selected eigenvalue is $\boldsymbol{a}_6$. Thus, the coefficients of ellipse are

$$
\begin{aligned}
a &= -0.05124; \\
b &= 0.0000477; \\
c &= -0.05095; \\
d &= -0.000017; \\
e &= -0.00018; \\
f &= 0.997386
\end{aligned}
$$

4.2.2 Ellipticity

The semimajor and semiminor axes of ellipse can be figured out by calculating the coefficients of the ellipse. Then, the ratio of A/B can be found. When the ratios of the two runs are compared, the change in ellipticity can be determined.

Since the semimajor and semiminor axes of ellipse may take an angle with x-y axes of rectangular coordinate and the origin of ellipse may not be at the origin of rectangular coordinate, Eq. 2.21 must be simplified by rotation and translation of axes. Then, the lengths of semimajor to semiminor axes can be easily determined.

The coefficients of ellipse shown in Section 4.2.1 are used as an example to calculate the ratio of A/B of the ellipse as follows:

From Eq. 2.21, the general conic equation of an implicit second order polynomial is

$$ax^2 + bxy + cy^2 + dx + ey + f = 0 \qquad (2.21)$$

The coefficients of ellipse calculated in Section 4.2.1 are

$$
\left.
\begin{aligned}
a &= -0.05124; \quad & b &= 0.0000477; \\
c &= -0.05095; \quad & d &= -0.000017; \\
e &= -0.00018; \quad & f &= 0.997386
\end{aligned}
\right\} \qquad (4.10)
$$

Substituting the coefficients of ellipse into Eq. 2.21, we obtained

$$-0.05124x^2 + 0.0000477xy - 0.05095y^2 - 0.000017x - 0.00018y + 0.997386 = 0 \quad (4.11)$$

(1) Simplification by rotating axes

Substituting Eq. 4.10 into Eq. 2.60 and Eq. 2.61, we get

$$cos2\theta = \frac{[\,(-0.05124) - (-0.05095)\,]}{([-0.05124) - (-0.05095)]^2 + 0.0000477^2)^{1/2}} = -0.986741147 \quad (4.12)$$

$$sin2\theta = \frac{0.0000477}{([-0.05124) - (-0.05095)]^2 + 0.0000477^2)^{1/2}} = 0.162301906 \quad (4.13)$$

Substituting Eq. 4.12 into Eq. 2.62 and Eq. 2.63, we have

$$cos\theta = ((1 + (-6.079665)) / 2)^{1/2} = 0.08142129 \quad (4.14)$$

$$sin\theta = ((1 - (-6.079665)) / 2)^{1/2} = 0.996679775 \quad (4.15)$$

Substituting Eq. 4.10, Eq. 4.12, Eq. 4.13, Eq. 4.14 and Eq. 4.15 into Eq. 2.53 through Eq. 2.58, we get the coefficients a', b', c', d', e', and f' in (x′ - y′) coordinate which are

$$\begin{aligned} a' &= (-0.05124 * 0.08142129^{\,2}) + \\ &\quad (0.0000477 * 0.996679775 * 0.08142129) + \\ &\quad (-0.05095 * 0.996679775^{\,2}) \\ &= -0.0509481 \end{aligned} \quad (4.16)$$

$$\begin{aligned} b' &= (0.0000477)*(-0.986741147) + \\ &\quad (-0.05095 - (-0.05124)) * (0.162301906) \\ &= 0.0000000 \end{aligned} \quad (4.17)$$

$$\begin{aligned} c' &= (-0.05124 * 0.996679775^{\,2}) - \\ &\quad (0.0000477 * 0.996679775 * 0.08142129) + \\ &\quad (-0.05095 * 0.08142129^{\,2}) \\ &= -0.0512419 \end{aligned} \quad (4.18)$$

$$d' = (-0.000017 * 0.08142129) + (-0.00018 * 0.996679775) = -0.0001808 \quad (4.19)$$

$$e' = (-0.00018 * 0.08142129) - (-0.000017 * 0.996679775) = 0.0000023 \quad (4.20)$$

$$f' = 0.997386 \quad (4.21)$$

Substituting Eq. 4.16 through Eq. 4.21 into Eq. 2.52, we get

$$-0.0509479x'^2 - 0.0512435y'^2 - 0.000185x' + 0.0000025y' + 0.99739 = 0 \quad (4.22)$$

Eq. 4.22 is simplified by rotating axes from x-y axes to x′-y′ axes as shown in Fig. 4.7.

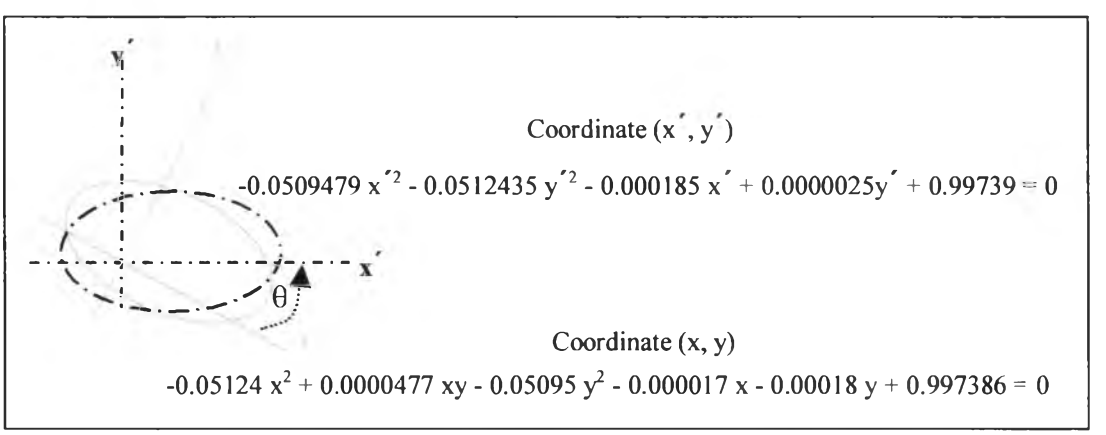

Figure 4.7: Simplification of equation by rotating axes.

(2) Simplification by translating axes

Substituting Eq. 4.16 through Eq. 4.21 into Eq. 2.73 and Eq. 2.74, we get

$$h = \frac{((2(-0.0512435)(-0.000185)) - (0*0.0000025))}{(0^2 - 4(-0.0509479)(-0.0512435))} = -0.001774224 \quad (4.23)$$

$$k = \frac{((2(-0.0509479)(0.0000025)) - (0*(-0.000185)))}{(0^2 - 4(-0.0509479)(-0.0512435))} = 0.00002232 \quad (4.24)$$

Substituting Eq. 4.16 through Eq. 4.21 and Eq. 4.23 through Eq. 4.24 into Eq. 2.65 through Eq. 2.70, we get the coefficients a'', b'', c'', d'', e'', and f'' in (x''-y'') coordinate which are

$$a'' = -0.0509479 \tag{4.25}$$

$$b'' = 0.00000 \tag{4.26}$$

$$c'' = -0.0512435 \tag{4.27}$$

$$\begin{aligned} d'' &= (2(-0.0509479)(-0.001774224)) + \\ &\quad (0(0.00002232)) + \\ &\quad (-0.000185) \\ &= 0.0000000 \end{aligned} \tag{4.28}$$

$$\begin{aligned} e'' &= (0(-0.001774224)) + \\ &\quad (2(-0.0512435)(0.00002232)) + \\ &\quad 0.0000025 \\ &= 0.0000000 \end{aligned} \tag{4.29}$$

$$\begin{aligned} f'' &= ((-0.0509479)(-0.001774224^{\,2})) + \\ &\quad (0(-0.001774224)(0.00002232)) + \\ &\quad ((-0.0512435)(0.00002232^{\,2}))+ \\ &\quad ((-0.000185)(-0.001774224)) + \\ &\quad ((0.0000025)(0.00002232)) + 0.99739 \\ &= 0.9973862 \end{aligned} \tag{4.30}$$

Substituting Eq. 4.25 through Eq. 4.30 into Eq. 2.64, we have

$$-0.0509479\, x''^2 - 0.0512435\, y''^2 + 0.99739 = 0 \tag{4.31}$$

Eq. 4.31 is simplified by translating axes from x'-y' axes to x''-y'' axes as shown in Fig. 4.8

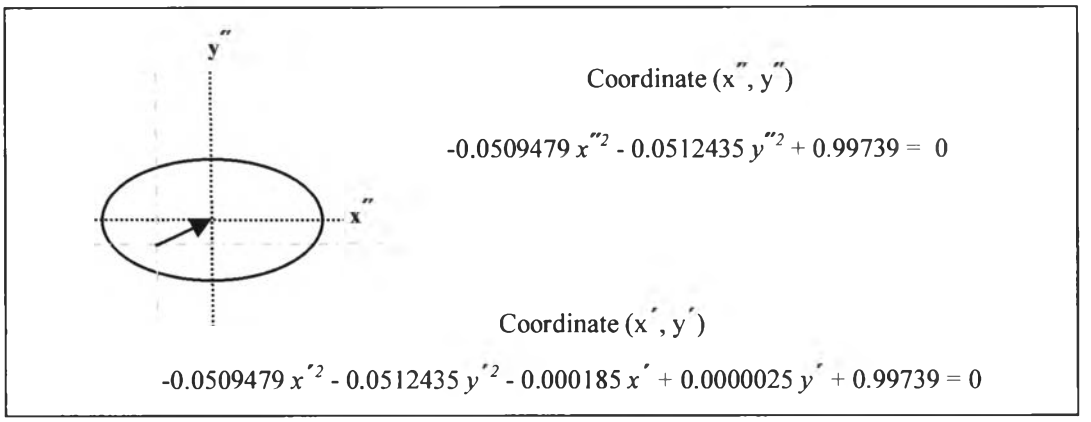

Figure 4.8: Simplification of equation by translating axes.

Eq. 4.31 is rearranged in the standard form as

$$(x''/ 4.4245)^2 + (y''/ 4.4118)^2 = 1 \qquad (4.32)$$

From Eq. 4.32, $A = 4.4245$ and $B = 4.4118$

Or A is calculated by substituting Eq. 4.25 and Eq. 4.30 into Eq. 2.76 as

$$A = -0.9973862 / -0.0509479$$
$$= 4.4245$$

And B is calculated by substituting Eq. 4.27 and Eq. 4.30 into Eq. 2.77 as

$$B = -0.9973862 / -0.0512435$$
$$= 4.4118$$

Substituting Eq. 4.25 and Eq. 4.27 into Eq. 2.79, the ratio of A/B is

$$A/B = -0.0512435 / -0.0509479$$
$$= 1.002896$$

Comparison between A/B ratios of two runs tells us whether the ellipticity of casing has changed or not. This change is the effect of the rock stress and strain. Table 4.4 shows that there is a small change of the ellipticity due to the stress and strain of rock on the casing.

Table 4.4: The A/B ratio of two runs.

Depth	Run 1			Run 2		
(ft)	*A*	*B*	*A/B*	*A*	*B*	*A/B*
2010.0	4.42454	4.41176	1.00290	4.43633	4.40512	1.00709
2009.5	4.42499	4.41363	1.00258	4.43315	4.41038	1.00516
2009.0	4.42383	4.41056	1.00301	4.43695	4.40759	1.00666
2008.5	4.42776	4.40920	1.00421	4.43996	4.40772	1.00731

4.2.3 Damage and scale identification

The casing damage and scale precipitation is shown by subtracting radii measurement (rectangular coordinate) from the center to the fitted ellipse curve for every position at the same depth as shown in Table 4.5.

Then, the distances between radii and ellipse curve as shown in Fig. 4.9 are plotted up using the function "imagesc" in MATLAB. We can visualize this image to find out where the location of the casing damage is.

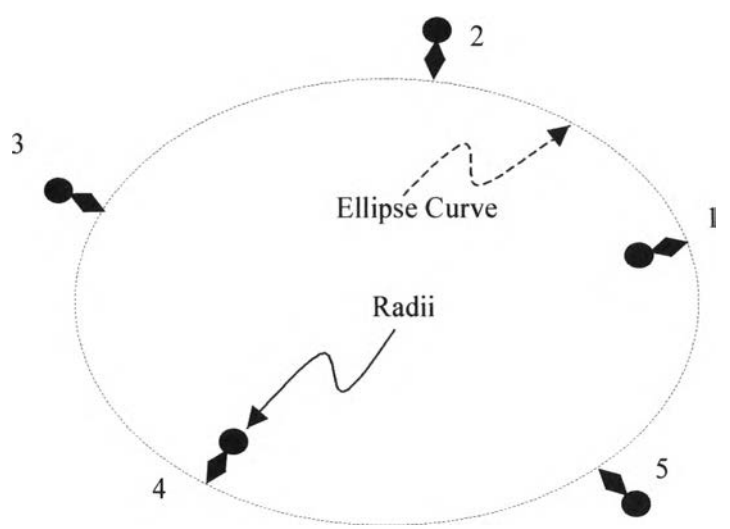

Figure 4.9: Distance between radii and ellipse curve.

As mentioned before, the casing shape is classified to circular and oval casing. We divide the damage and scale identification into 2 cases as follows:

Table 4.5: The distance between ellipse and radii at the depth 2010.0 ft of Run 2.

Position	Ellipse		Data		Distance between ellipse and radii
	x	y	x	y	
1	4.4129	0.3861	4.4252	0.3872	-0.0123
2	4.3640	0.7695	4.3686	0.7703	-0.0046
3	4.2814	1.1472	4.2868	1.1486	-0.0055
4	4.1658	1.5162	4.1700	1.5178	-0.0044
5	4.0181	1.8737	4.0374	1.8827	-0.0214
6	3.8393	2.2166	3.8491	2.2223	-0.0114
7	3.6310	2.5424	3.6302	2.5419	0.0010
8	3.3947	2.8485	3.3899	2.8444	0.0064
9	3.1325	3.1325	3.1416	3.1416	-0.0128
10	2.8464	3.3923	2.8510	3.3977	-0.0071
11	2.5388	3.6258	2.5339	3.6188	0.0086
12	2.2120	3.8313	2.2038	3.8171	0.0163
13	1.8687	4.0073	1.8705	4.0112	-0.0043
14	1.5115	4.1527	1.5121	4.1545	-0.0020
15	1.1432	4.2663	1.1402	4.2554	0.0113
16	0.7666	4.3475	0.7645	4.3355	0.0121
17	0.3846	4.3957	0.3847	4.3974	-0.0018
18	0.0000	4.4106	0.0000	4.4186	-0.0080
19	-0.3843	4.3923	-0.3839	4.3876	0.0048
20	-0.7654	4.3410	-0.7659	4.3439	-0.0029
21	-1.1407	4.2571	-1.1446	4.2715	-0.0150
22	-1.5073	4.1412	-1.5112	4.1520	-0.0115
23	-1.8625	3.9942	-1.8588	3.9863	0.0088
24	-2.2039	3.8172	-2.2055	3.8201	-0.0033
25	-2.5288	3.6115	-2.5332	3.6177	-0.0076
26	-2.8349	3.3785	-2.8328	3.3760	0.0033
27	-3.1199	3.1199	-3.1123	3.1123	0.0106
28	-3.3816	2.8375	-3.3792	2.8355	0.0032
29	-3.6180	2.5334	-3.6141	2.5306	0.0048
30	-3.8273	2.2097	-3.8074	2.1982	0.0231
31	-4.0078	1.8689	-3.9914	1.8612	0.0181
32	-4.1581	1.5134	-4.1434	1.5081	0.0156
33	-4.2768	1.1460	-4.2618	1.1420	0.0155
34	-4.3630	0.7693	-4.3447	0.7661	0.0185
35	-4.4158	0.3863	-4.4923	0.3930	-0.0767
36	-4.4348	0.0000	-4.5043	0.0000	-0.0695

Table 4.5: The distance between ellipse and radii at the depth 2010.0 ft of Run 2 (continued).

Position	Ellipse		Data		Distance between ellipse and radii
	x	y	x	y	
37	-4.4197	-0.3867	-4.4078	-0.3856	0.0119
38	-4.3705	-0.7706	-4.3606	-0.7689	0.0101
39	-4.2876	-1.1489	-4.2952	-1.1509	-0.0079
40	-4.1715	-1.5183	-4.1676	-1.5169	0.0042
41	-4.0233	-1.8761	-4.0176	-1.8734	0.0062
42	-3.8439	-2.2193	-3.8375	-2.2156	0.0074
43	-3.6350	-2.5453	-3.6419	-2.5501	-0.0084
44	-3.3982	-2.8514	-3.3895	-2.8441	0.0114
45	-3.1354	-3.1354	-3.1229	-3.1229	0.0176
46	-2.8487	-3.3949	-2.8417	-3.3866	0.0109
47	-2.5405	-3.6281	-2.5425	-3.6310	-0.0035
48	-2.2132	-3.8333	-2.2064	-3.8216	0.0135
49	-1.8694	-4.0089	-1.8614	-3.9918	0.0189
50	-1.5118	-4.1538	-1.5083	-4.1441	0.0103
51	-1.1433	-4.2668	-1.1455	-4.2752	-0.0086
52	-0.7666	-4.3474	-0.7663	-4.3460	0.0014
53	-0.3845	-4.3950	-0.3838	-4.3871	0.0080
54	0.0000	-4.4094	0.0000	-4.4096	-0.0003
55	0.3841	-4.3905	0.3857	-4.4090	-0.0186
56	0.7650	-4.3386	0.7675	-4.3526	-0.0142
57	1.1399	-4.2542	1.1436	-4.2682	-0.0144
58	1.5061	-4.1379	1.5108	-4.1509	-0.0139
59	1.8608	-3.9906	1.8679	-4.0057	-0.0167
60	2.2016	-3.8133	2.2049	-3.8191	-0.0066
61	2.5260	-3.6075	2.5284	-3.6110	-0.0043
62	2.8315	-3.3744	2.8290	-3.3715	0.0038
63	3.1158	-3.1158	3.1174	-3.1174	-0.0022
64	3.3769	-2.8336	3.3684	-2.8264	0.0112
65	3.6128	-2.5297	3.6145	-2.5309	-0.0021
66	3.8216	-2.2064	3.8118	-2.2007	0.0114
67	4.0017	-1.8660	3.9884	-1.8598	0.0147
68	4.1516	-1.5111	4.1287	-1.5027	0.0244
69	4.2701	-1.1442	4.2690	-1.1439	0.0011
70	4.3561	-0.7681	4.3455	-0.7662	0.0108
71	4.4089	-0.3857	4.4022	-0.3851	0.0067
72	4.4279	0.0000	4.4198	0.0000	0.0081

(a) Circular casing

Case 1a: No casing damage and scale precipitation

The ellipse fit algorithm was used to process the data in Run 1 shown in Table 4.1 when the casing shape is circular. The differences between the raw radii and the ellipse curve are shown in Fig. 4.10. As seen in the figure, there is no casing damage and scale precipitation observed during Run 1.

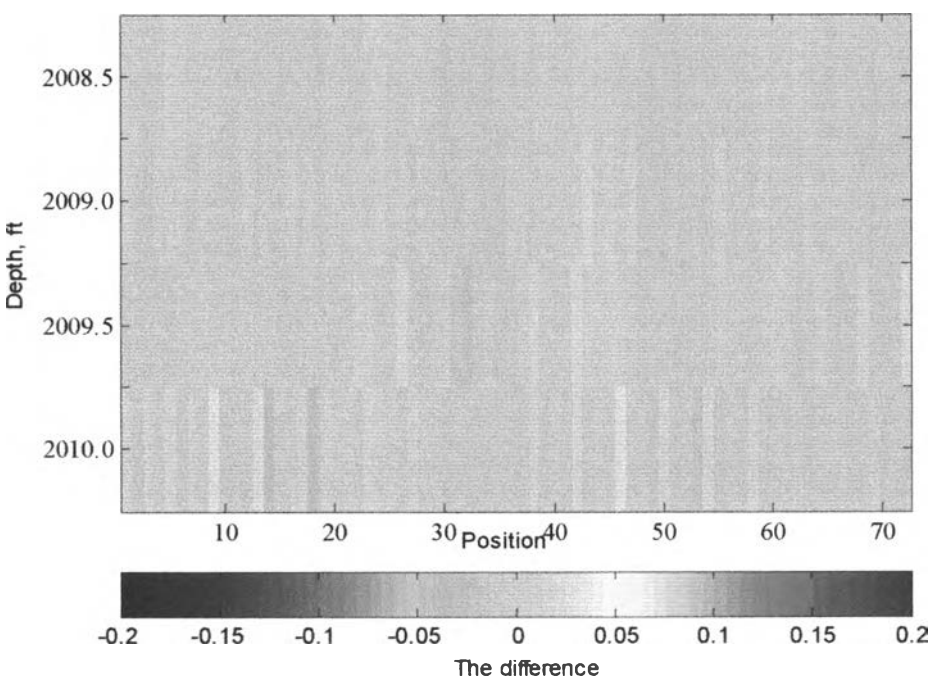

Figure 4.10: Damage identification of Run 1 processed by the ellipse fit algorithm (circular casing).

Therefore, comparing the results shown in Figs. 4.2 and 4.10, It can be seen that both the vector sum and the ellipse fit algorithms can correctly identify the location of casing wear in case of circular casing, both the vector sum and the ellipse fit algorithms are applicable.

Case 2a: Casing is damaged

The ellipse fit algorithm was used to process the data in Run 2 shown in Table 4.1 when the casing shape is circular. The differences between the raw radii and the ellipse curve are shown in Fig. 4.11. As seen in the figure, there is a damage in the second run.

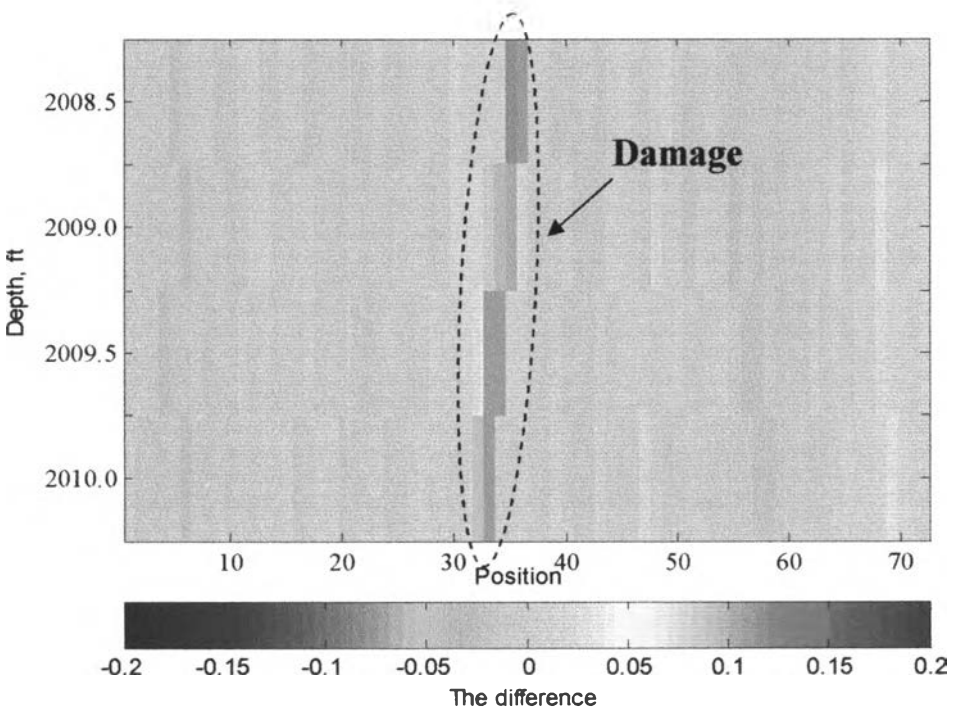

Figure 4.11: Damage identification of Run 2 processed by the ellipse fit algorithm (circular casing).

Therefore, comparing the results shown in Figs. 4.3 and 4.11, It can be seen that both the vector sum and the ellipse fit algorithms can correctly identify the location of casing wear in case of circular casing, both the vector sum and the ellipse fit algorithms are applicable.

In case of the circular casing, the ellipticity is approximately 1.00. Thus, if the ellipticity is equal to 1.00, both the vector sum and the ellipse fit algorithms are applicable.

(b) Oval casing

Case 1b: No casing damage and scale precipitation

The ellipse fit algorithm was used to process the measurements in Run 1 shown in Table 4.2 when the casing shape is oval. The differences between the raw radii and the ellipse curve are shown in Fig. 4.12.

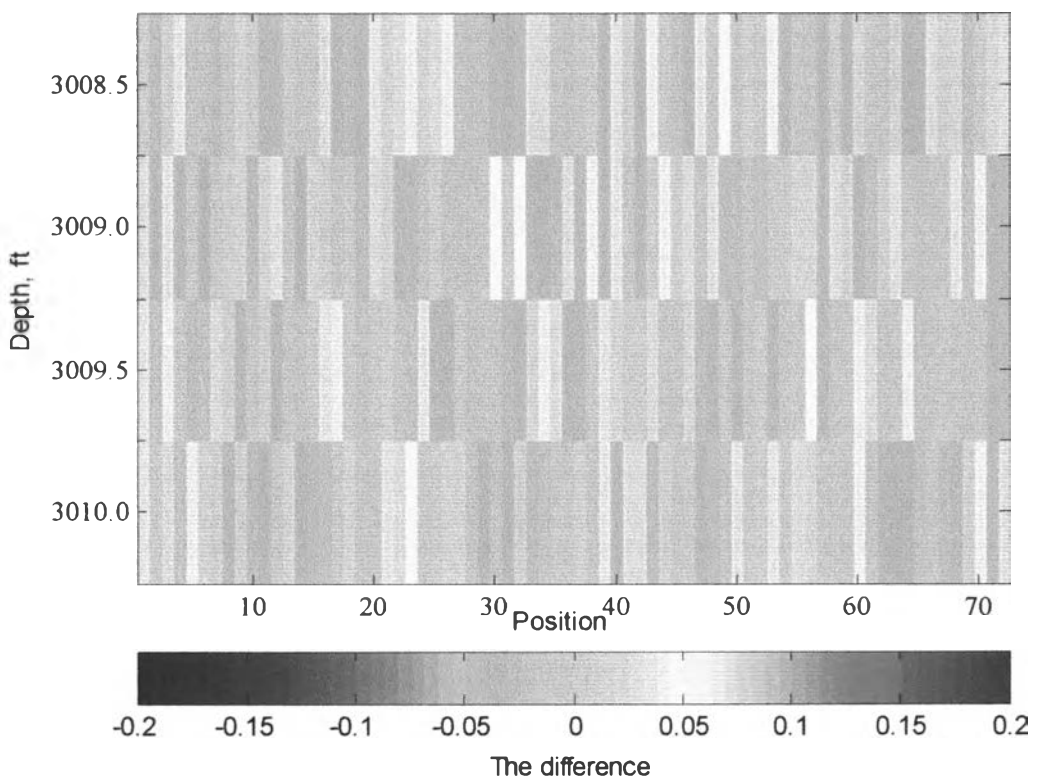

Figure 4.12: Damage identification of Run 1 processed by the ellipse fit algorithm (oval casing).

Unlike the results obtained from the vector sum algorithm shown in Fig. 4.4, the results obtained from the ellipse fit algorithm shown in Fig. 4.12 clearly illustrates that these are no damages or precipitations in the casing. The ellipse fit algorithm is suitable for oval casing because the ellipse fit algorithm fits the data with an elliptical curve.

Case 2b: Casing is damaged

The ellipse fit algorithm was used to process the measurements in Run 2 shown in Table 4.2 when the casing shape is oval. The differences between the raw radii and the ellipse curve are shown in Fig. 4.13.

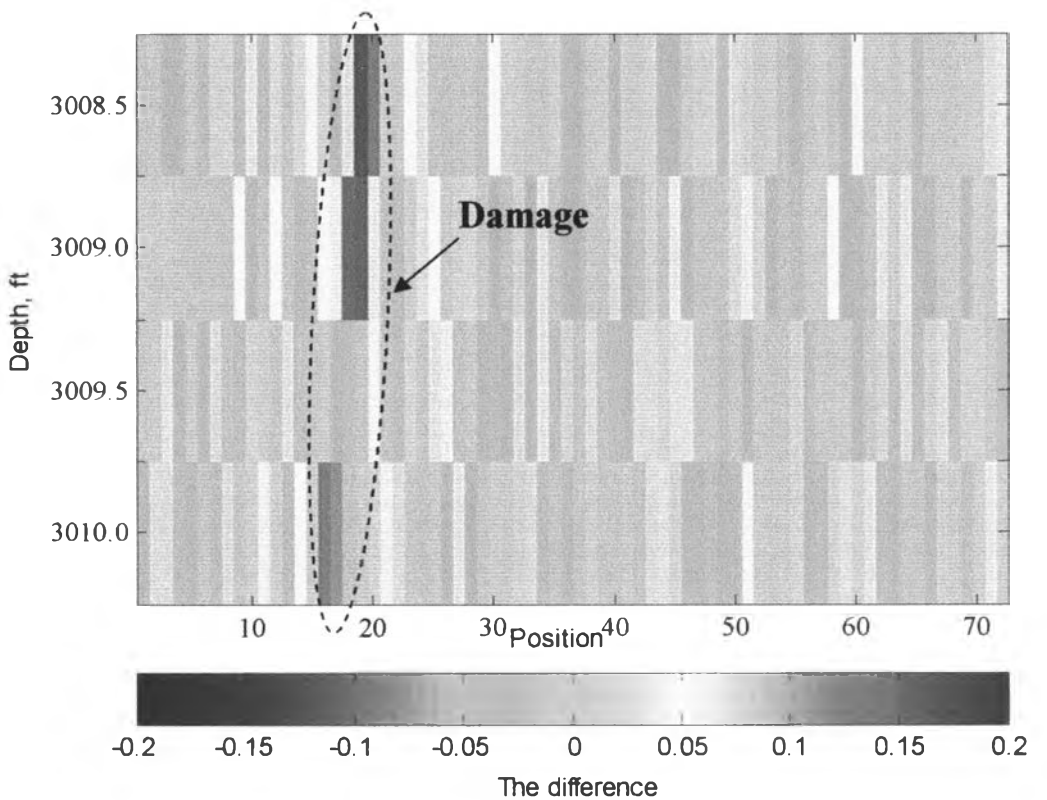

Figure 4.13: Damage identification of Run 2 processed by the ellipse fit algorithm (oval casing).

Unlike the results obtained from the vector sum algorithm shown in Fig. 4.5, the ellipse fit algorithm correctly identifies the location of damage without any false identification as seen in Fig. 4.13. Since the ellipse fit algorithm assumes the casing shape to be elliptical, the algorithm can handle oval-shape casing better than the vector sum algorithm.

In case of the oval casing, the ellipticity is approximately 1.02. Thus, if the ellipticity is equal to 1.02 approximately, only the ellipse fit algorithm are applicable.

4.3 Dealing with Missing Data

The vector sum algorithm has some drawbacks, especially, when some of the measurements are missing. Sometimes the data value may not be valid at a certain positions due to bad signals. In this case, the tool records -999.25 as an output so that computer programs can identify that this measurement is not valid.

To illustrate how a missing data point can affect the relocation of the tool center, let's assume that the caliper tool measures only 4 positions of casing radii and that the fourth position is not valid as shown in Fig. 4.14. And let's assume that each radius has a magnitude of 4 units.

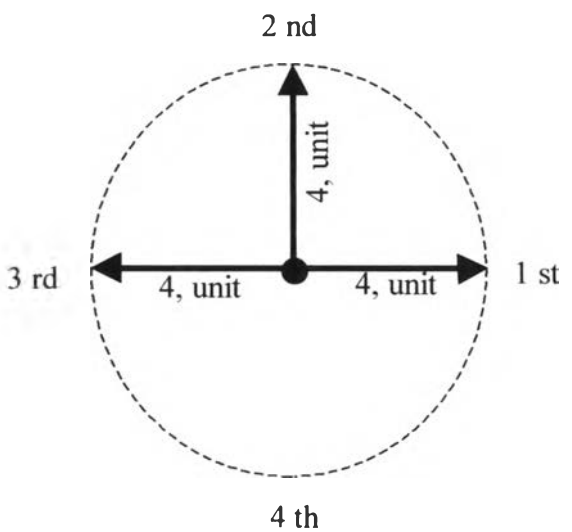

Figure 4.14: The data value is not valid at forth position.

After applying the vector sum algorithm, the tool center is moved in the direction opposite to the location where the data point is missing as shown in Fig. 4.15.

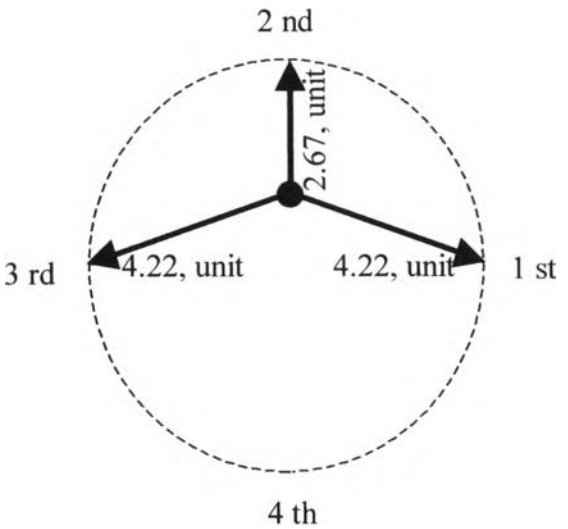

Figure 4.15: Tool center after applying the vector sum algorithm.

Fig. 4.15 shows that there are two damages of the casing, i.e., the first and third position and a scale at the second position. The fact is that are no scale or damages at all.

Case 1: Missing data processed by the vector sum algorithm

The vector sum algorithm was used to process the measurements in Run 2 shown in Table 4.1. In this case, data are assumed to be missing at positions 68-72 at depth 2008.5 ft., positions 67-71 at depth 2009.0 ft., positions 66-70 at depth 2009.5 ft. and positions 65-69 at depth 2010.0 ft. The differences between the corrected radii and the average radius determined from the vector sum algorithm are shown in Fig. 4.16. As seen in the figure, there are damage and scale precipitation zones in this run. In case of complete data set for this example, there is only one damage at positions 32-36 as shown in Fig. 4.3.

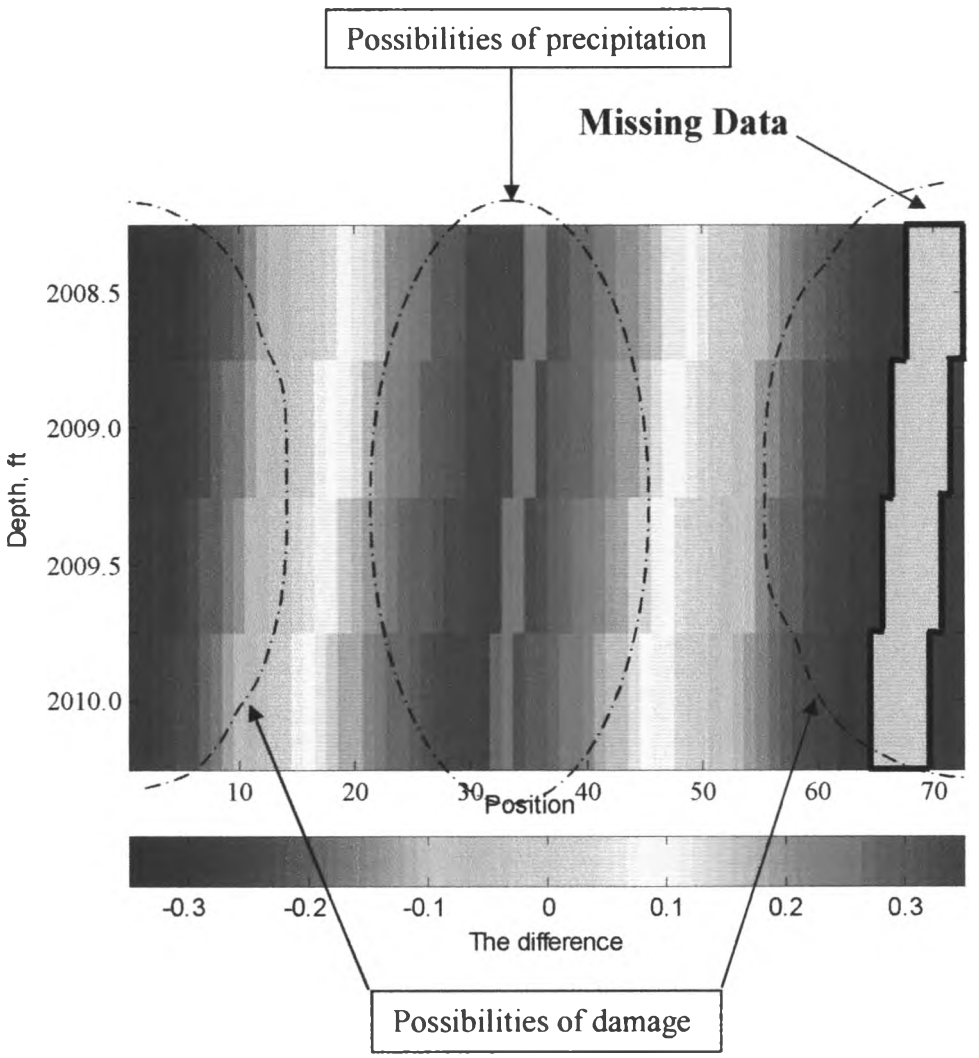

Figure 4.16: Damage and scale identification using the vector sum algorithm when some data are missing.

However, if the missing data are replaced with the internal radius of the casing, there is no false identification of scale precipitation. The results are shown in Fig. 4.17.

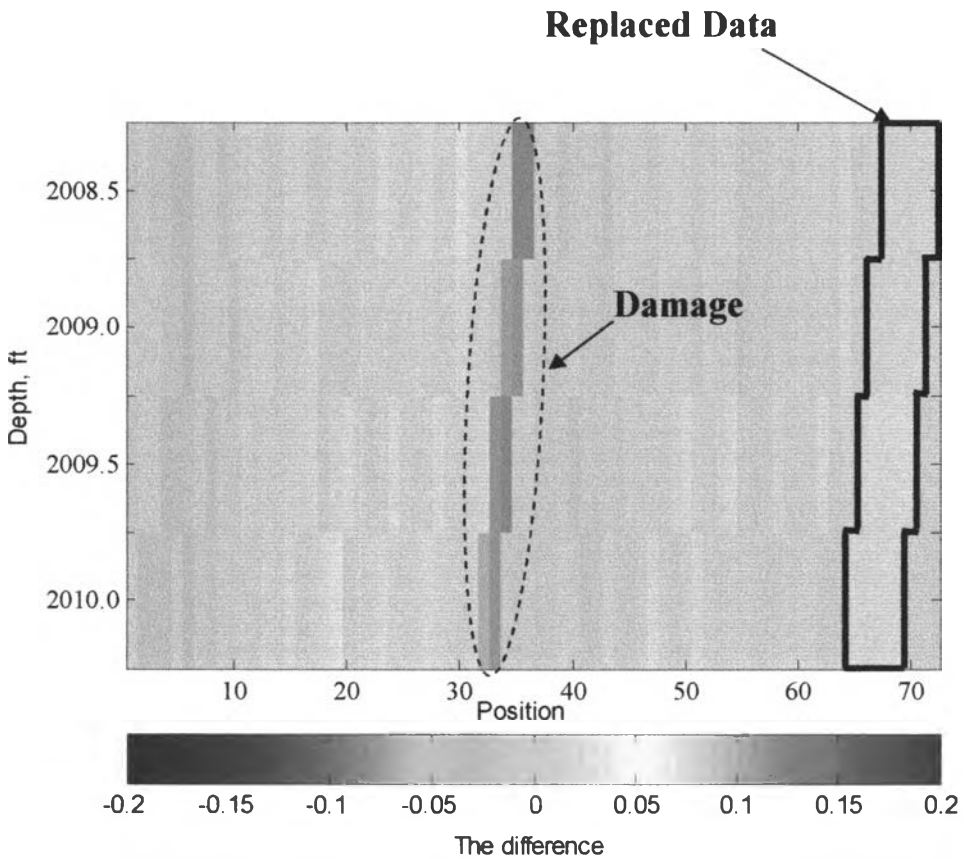

Figure 4.17: Damage and scale identification using the vector sum algorithm when the missing data are replaced with the internal radius of the casing.

Case 2: Missing data processed by the ellipse fit algorithm

The ellipse fit algorithm was used to process the measurements in Run 2 shown in Table 4.1. In this case, data are assumed to be missing at positions 68-72 at depth 2008.5 ft., positions 67-71 at depth 2009.0 ft., positions 66-70 at depth 2009.5 ft. and positions 65-69 at depth 2010.0 ft. The differences between the raw radii and the ellipse curve obtained from the ellipse fit algorithm are shown in Fig. 4.18. As seen in the figure, the ellipse fit algorithm correctly identifies the position of damage even though some of the data are missing.

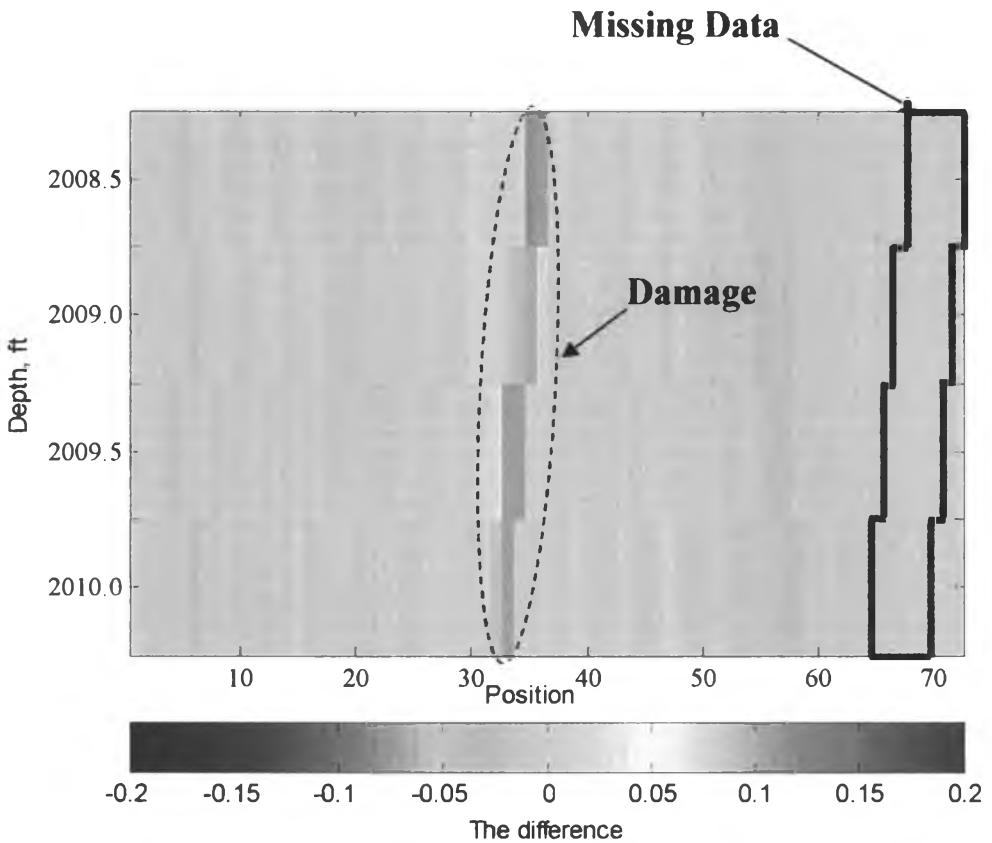

Figure 4.18: Damage and scale identification using the ellipse fit algorithm when some data are missing.

These two examples show that the vector sum algorithm is not applicable when data are missing. This problem can be overcome when the missing data are replaced with the internal radius of the casing. Even though some of the data are missing, the ellipse fit algorithm can process the data accurately because the ellipse fit uses the elliptic equation to fit the data via least squares regression.

In case of oval casing, the vector sum algorithm is not applicable because there is false identification as shown in Fig. 4.6

4.4 Synchronization of measurements obtained in two runs

In an attempt to reduce cost, we will not use the deviation sensor in the second run of caliper log. In this case, there is a need to synchronize the data obtained from the two runs. Since we have illustrated the benefits of the ellipse fit algorithm over the vector sum algorithm, we chose to process the data using the ellipse fit algorithm. In this section, we will discuss how to synchronize the data obtained from two runs made at different times when the ellipse fit algorithm is used.

When the coefficients of the general conic equation for both data sets are calculated, the positions between two runs are synchronized by shifting the data positions and determining the minimum of the sum of errors (differences between coefficients of Run 1 and those of Run 2) over all depths. In each shift, the sum of the absolute of the differences between the coefficients (error) at any depth is calculated as shown in Eq. 3.1

$$\text{error} = |a_1 - a_2| + |b_1 - b_2| + |c_1 - c_2| + |d_1 - d_2| + |e_1 - e_2| + |f_1 - f_2| \tag{3.1}$$

Table 4.6 shows the sum of the absolute of the differences between the coefficients (error) of the ellipse fitted to data obtained from two runs at depth 2010.0 ft. The lowest error for this depth is 11.61 which is obtained in the 60^{th} rotation.

Table 4.6: The sum of the absolute of the differences between the coefficients (error).

Rotation	At depth 2010.0 ft						
	$a_1 - a_2$	$b_1 - b_2$	$c_1 - c_2$	$d_1 - d_2$	$e_1 - e_2$	$f_1 - f_2$	error
1	0.00878	-10.015	-0.0066	-19.135	1.3505	-0.0000057	30.52
2	0.00960	-8.052	-0.0074	-18.736	1.5152	-0.0000057	28.32
3	0.01024	-5.814	-0.0080	-18.186	1.6759	-0.0000057	25.69
4	0.01070	-3.369	-0.0085	-17.490	1.8315	-0.0000057	22.71
5	0.01095	-0.791	-0.0088	-16.654	1.9808	-0.0000057	19.45
6	0.01099	1.841	-0.0088	-15.683	2.1227	-0.0000057	19.67
7	0.01081	4.447	-0.0086	-14.585	2.2559	-0.0000057	21.31
8	0.01043	6.949	-0.0082	-13.369	2.3797	-0.0000057	22.72
9	0.00985	9.271	-0.0077	-12.043	2.4929	-0.0000057	23.82
10	0.00909	11.340	-0.0069	-10.618	2.5948	-0.0000057	24.57
11	0.00818	13.096	-0.0060	-9.105	2.6845	-0.0000057	24.90
12	0.00714	14.484	-0.0049	-7.514	2.7614	-0.0000056	24.77
13	0.00600	15.463	-0.0038	-5.859	2.8249	-0.0000056	24.16
14	0.00480	16.002	-0.0026	-4.152	2.8745	-0.0000056	23.04
15	0.00358	16.085	-0.0013	-2.405	2.9098	-0.0000056	21.40
16	0.00236	15.710	-0.0001	-0.633	2.9306	-0.0000056	19.28
17	0.00120	14.888	0.0011	1.152	2.9368	-0.0000056	18.98
18	0.00012	13.643	0.0021	2.936	2.9281	-0.0000057	19.51
19	-0.00085	12.015	0.0031	4.705	2.9048	-0.0000057	19.63
20	-0.00166	10.052	0.0039	6.446	2.8670	-0.0000057	19.37
21	-0.00231	7.814	0.0046	8.145	2.8150	-0.0000057	18.78
22	-0.00276	5.369	0.0050	9.790	2.7492	-0.0000057	17.92
23	-0.00302	2.791	0.0053	11.368	2.6701	-0.0000057	16.84
24	-0.00305	0.159	0.0053	12.867	2.5783	-0.0000057	15.61
25	-0.00288	-2.447	0.0052	14.276	2.4744	-0.0000057	19.21
26	-0.00250	-4.949	0.0048	15.584	2.3593	-0.0000057	22.90
27	-0.00192	-7.271	0.0042	16.781	2.2339	-0.0000057	26.29
28	-0.00116	-9.340	0.0034	17.857	2.0991	-0.0000057	29.30
29	-0.00025	-11.096	0.0025	18.806	1.9559	-0.0000057	31.86
30	0.00080	-12.484	0.0015	19.619	1.8055	-0.0000056	33.91
31	0.00193	-13.463	0.0003	20.290	1.6489	-0.0000056	35.40
32	0.00313	-14.002	-0.0009	20.814	1.4874	-0.0000056	36.31
33	0.00436	-14.085	-0.0021	21.188	1.3221	-0.0000056	36.60
34	0.00557	-13.710	-0.0033	21.408	1.1545	-0.0000056	36.28
35	0.00674	-12.888	-0.0045	21.473	0.9856	-0.0000056	35.36
36	0.00782	-11.643	-0.0056	21.381	0.8169	-0.0000057	33.86
37	0.00878	-10.015	-0.0066	21.135	0.6495	-0.0000057	31.82
38	0.00960	-8.052	-0.0074	20.736	0.4848	-0.0000057	29.29
39	0.01024	-5.814	-0.0080	20.186	0.3241	-0.0000057	26.34
40	0.01070	-3.369	-0.0085	19.490	0.1685	-0.0000057	23.05
41	0.01095	-0.791	-0.0088	18.654	0.0192	-0.0000057	19.48
42	0.01099	1.841	-0.0088	17.683	-0.1227	-0.0000057	19.67

Table 4.6: The sum of the absolute of the differences between the coefficients (error) (continued).

Rotation	At depth 2010.0 ft						
	$a_1 - a_2$	$b_1 - b_2$	$c_1 - c_2$	$d_1 - d_2$	$e_1 - e_2$	$f_1 - f_2$	error
43	0.01081	4.447	-0.0086	16.585	-0.2559	-0.0000057	21.31
44	0.01043	6.949	-0.0082	15.369	-0.3797	-0.0000057	22.72
45	0.00985	9.271	-0.0077	14.043	-0.4929	-0.0000057	23.82
46	0.00909	11.340	-0.0069	12.618	-0.5948	-0.0000057	24.57
47	0.00818	13.096	-0.0060	11.105	-0.6845	-0.0000057	24.90
48	0.00714	14.484	-0.0049	9.514	-0.7614	-0.0000056	24.77
49	0.00600	15.463	-0.0038	7.859	-0.8249	-0.0000056	24.16
50	0.00480	16.002	-0.0026	6.152	-0.8745	-0.0000056	23.04
51	0.00358	16.085	-0.0013	4.405	-0.9098	-0.0000056	21.40
52	0.00236	15.710	-0.0001	2.633	-0.9306	-0.0000056	19.28
53	0.00120	14.888	0.0011	0.848	-0.9368	-0.0000056	16.67
54	0.00012	13.643	0.0021	-0.936	-0.9281	-0.0000057	15.51
55	-0.00085	12.015	0.0031	-2.705	-0.9048	-0.0000057	15.63
56	-0.00166	10.052	0.0039	-4.446	-0.8670	-0.0000057	15.37
57	-0.00231	7.814	0.0046	-6.145	-0.8150	-0.0000057	14.78
58	-0.00276	5.369	0.0050	-7.790	-0.7492	-0.0000057	13.92
59	-0.00302	2.791	0.0053	-9.368	-0.6701	-0.0000057	12.84
60	**-0.00305**	**0.159**	**0.0053**	**-10.867**	**-0.5783**	**-0.0000057**	**11.61**
61	-0.00288	-2.447	0.0052	-12.276	-0.4744	-0.0000057	15.21
62	-0.00250	-4.949	0.0048	-13.584	-0.3593	-0.0000057	18.90
63	-0.00192	-7.271	0.0042	-14.781	-0.2339	-0.0000057	22.29
64	-0.00116	-9.340	0.0034	-15.857	-0.0991	-0.0000057	25.30
65	-0.00025	-11.096	0.0025	-16.806	0.0441	-0.0000057	27.95
66	0.00080	-12.484	0.0015	-17.619	0.1945	-0.0000056	30.30
67	0.00193	-13.463	0.0003	-18.290	0.3511	-0.0000056	32.11
68	0.00313	-14.002	-0.0009	-18.814	0.5126	-0.0000056	33.33
69	0.00436	-14.085	-0.0021	-19.188	0.6779	-0.0000056	33.96
70	0.00557	-13.710	-0.0033	-19.408	0.8455	-0.0000056	33.97
71	0.00674	-12.888	-0.0045	-19.473	1.0144	-0.0000056	33.39
72	0.00782	-11.643	-0.0056	-19.381	1.1831	-0.0000057	32.22

The rotation (among the 72 shifts) at which the error is lowest is the position at which the measurements from the two runs synchronize. Since the tool may spin during measurements made at different depths, the best fitted rotation may be different from depth to depth. Table 4.7 illustrates the best fitted rotation from depth 2008.5 ft to 2010.0 ft.

Table 4.7: The sum of the absolute of the differences between the coefficients at different depths.

Rotation	Depth (ft)			
	2010.0	2009.5	2009.0	2008.5
1	30.52	7.55	5.49	7.26
2	28.32	7.09	5.10	4.35
3	25.69	6.65	5.39	**1.51**
4	22.71	7.37	5.66	4.74
5	19.45	8.06	5.89	7.91
6	19.67	8.70	6.07	10.93
7	21.31	9.28	6.19	13.69
8	22.72	9.77	6.24	16.13
9	23.82	10.15	6.21	18.16
10	24.57	10.42	6.09	19.74
11	24.90	10.56	6.18	20.80
12	24.77	10.57	6.75	21.34
13	24.16	10.43	7.23	21.32
14	23.04	10.14	7.62	20.75
15	21.40	9.72	7.92	19.67
16	19.28	9.16	8.12	18.08
17	18.98	8.48	8.22	16.06
18	19.51	8.08	8.24	13.66
19	19.63	7.68	8.18	10.95
20	19.37	7.19	8.05	8.02
21	18.78	6.60	7.86	4.97
22	17.92	5.96	7.62	4.34
23	16.84	5.27	7.35	7.45
24	15.61	4.63	7.06	10.39
25	19.21	5.17	7.56	13.08
26	22.90	5.62	8.04	15.42
27	26.29	5.96	8.42	17.36
28	29.30	6.20	8.70	18.82
29	31.86	6.30	8.86	19.78
30	33.91	6.27	8.91	20.19
31	35.40	6.11	8.84	20.04
32	36.31	5.80	8.64	19.35
33	36.60	5.35	8.33	18.12
34	36.28	4.77	7.90	16.39
35	35.36	4.15	7.36	14.22
36	33.86	3.91	6.73	11.67
37	31.82	3.55	6.02	8.81
38	29.29	3.09	5.43	5.74
39	26.34	**2.65**	5.52	2.72
40	23.05	3.37	5.66	5.76
41	19.48	4.06	5.89	8.74
42	19.67	4.70	6.07	11.55

Table 4.7: The sum of the absolute of the differences between the coefficients at different depths (continued).

Rotation	Depth (ft)			
	2010.0	2009.5	2009.0	2008.5
43	21.31	5.28	6.19	14.11
44	22.72	5.77	6.24	16.33
45	23.82	6.15	6.21	18.16
46	24.57	6.55	6.09	19.52
47	24.90	7.21	5.87	20.38
48	24.77	7.75	5.56	20.70
49	24.16	8.16	5.16	20.49
50	23.04	8.42	4.66	19.73
51	21.40	8.54	4.07	18.45
52	19.28	8.52	4.12	16.69
53	16.67	8.36	4.22	14.50
54	15.51	8.08	4.24	11.94
55	15.63	7.68	4.18	9.09
56	15.37	7.19	4.05	6.04
57	14.78	6.60	3.86	2.87
58	13.92	5.96	3.62	2.14
59	12.84	5.27	3.51	5.17
60	**11.61**	4.63	**3.42**	8.05
61	15.21	5.17	4.13	10.69
62	18.90	5.62	4.83	13.01
63	22.29	5.96	5.45	15.01
64	25.30	6.20	5.97	16.56
65	27.95	6.81	6.38	17.59
66	30.30	7.37	6.68	18.08
67	32.11	7.81	6.86	18.01
68	33.33	8.10	6.92	17.39
69	33.96	8.26	6.85	16.24
70	33.97	8.27	6.67	14.60
71	33.39	8.15	6.37	12.50
72	32.22	7.91	5.98	10.03

Table 4.7 shows that at depth 2010.0 ft the 60^{th} rotation yields the lowest sum of the absolute of the coefficients, at depth 2009.5 ft the 39^{th} rotation yields the lowest sum of the absolute of the coefficients, at depth 2009.0 ft the 60^{th} rotation yields the lowest sum of the absolute of the coefficients, and at depth 2008.5 ft the 3^{rd} rotation yields the lowest sum of the absolute of the coefficients.

Radii measurements at depth 2010.0 ft, before synchronization from Run 1 and Run 2 are compared as shown in Fig. 4.19. After synchronization, the 60^{th} position of Run 2 is matched with the first position of Run 1 as shown in Fig. 4.20.

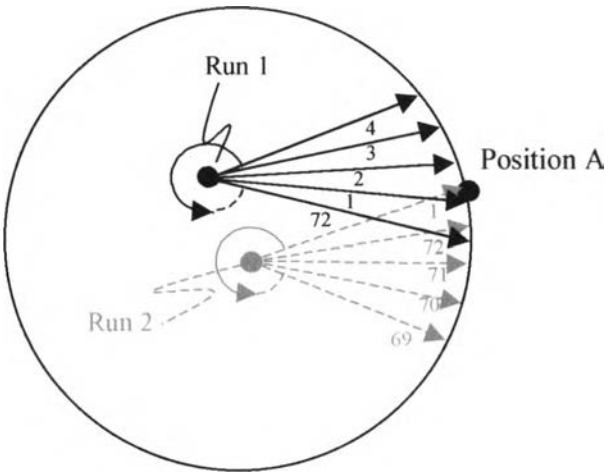

Figure 4.19: Radii measurements from two runs are compared before synchronization.

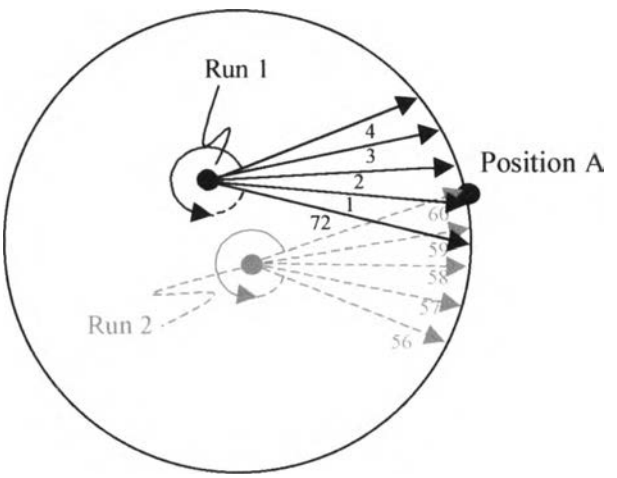

Figure 4.20: Radii measurements from two runs are compared after synchronization.

After synchronizing the two sets of measurements, the radii measurements from both runs can be compared to identify the location of casing wear or scale precipitation. However, we cannot verify the accuracy of the synchronization process since we don't know the exact orientation of the tool in the second run. In this study, we simply present an idea on how to synchronize between measurements when the deviation sensor is not lowered into the wellbore in the second run of caliper log. In order to study the effectiveness of the procedure, further investigation is needed.